Measurement of beam and target polarization observables in $\vec{\gamma}\vec{p} \rightarrow p\pi^+\pi^-$ using the CLAS spectrometer at Jefferson Lab

Sungkyun Park

Florida State University
Department of Physics

July 01, 2013
Dissertation Defense

Outline

Outline

1. Introduction
   - Baryon Spectroscopy
   - Why is $\pi^+\pi^-$ photoproduction needed ?
2. FROST Experiment
   - Jefferson Laboratory in Newport News, VA
   - Experimental devices for the FROST experiment
3. Data Analysis
   - Kinematic variables
   - Previous measurements
   - Basic event selection
4. Preliminary Results
   - Polarization Observable $\mathbf{I}^{\odot}$
   - Q-factor method : Event-based background subtraction
   - Polarization Observable $\mathbf{P_z}$
   - Polarization Observable $\mathbf{P_z^{\odot}}$
5. Summary

What are hadrons?

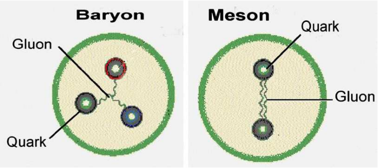

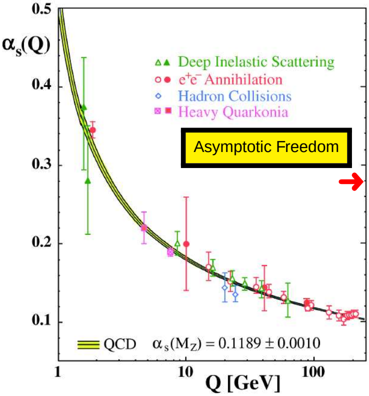

- Hadrons are composed of quarks bound by the strong interaction.
  - Baryon: qqq
  - Meson: $q\bar{q}$
- Quantum Chromodynamics (QCD)
  - QCD is the theory of strong interactions; the strong force describes the interactions of quarks and gluons making up hadrons.
- Strong interaction processes at larger distances and at small (soft) momentum transfers belong to the realm of non-perturbative QCD.
  - Constituent quark models are the most successful models for making predictions about the properties of baryon resonances in the non-perturbative region of QCD.

The N^* Program in JLab

➜ The study of the properties of baryon resonances

The spectrum of N^* resonances

Constituent quark model: Gluon-exchange model

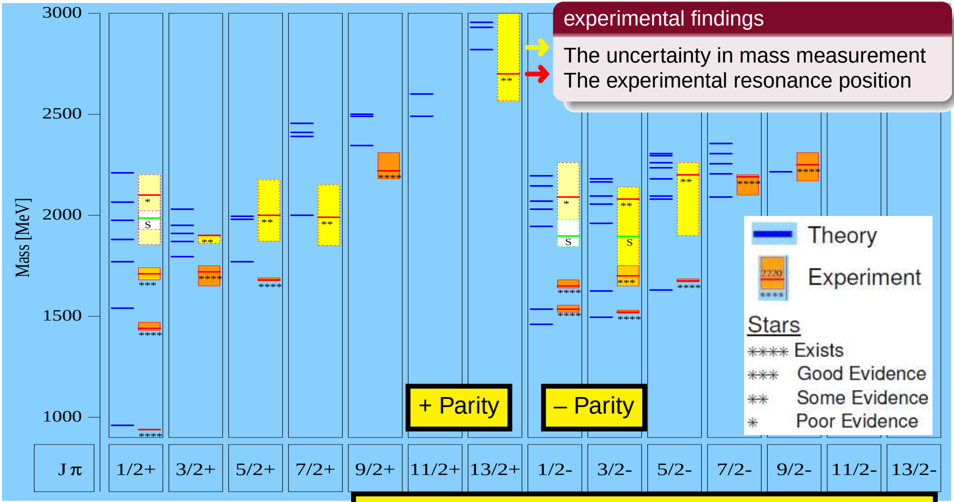

experimental findings

The uncertainty in mass measurement
The experimental resonance position

—— S. Capstick and N. Isgur, Phys. Rev. **D34** (1986) 2809

The spectrum of N^* resonances

Constituent quark model: N^* resonances (Isospin $\frac{1}{2}$)

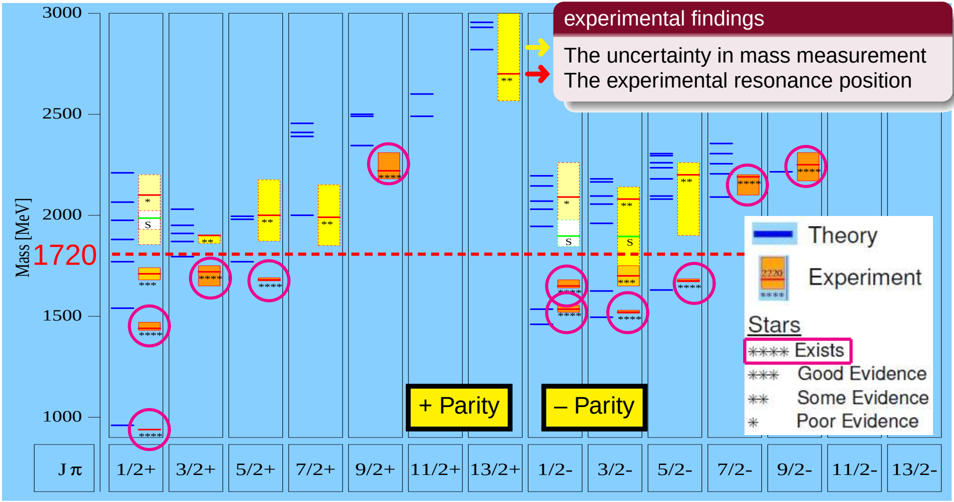

experimental findings

The uncertainty in mass measurement
The experimental resonance position

The spectrum of N^* resonances

Constituent quark model: N^* resonances (Isospin $\frac{1}{2}$)

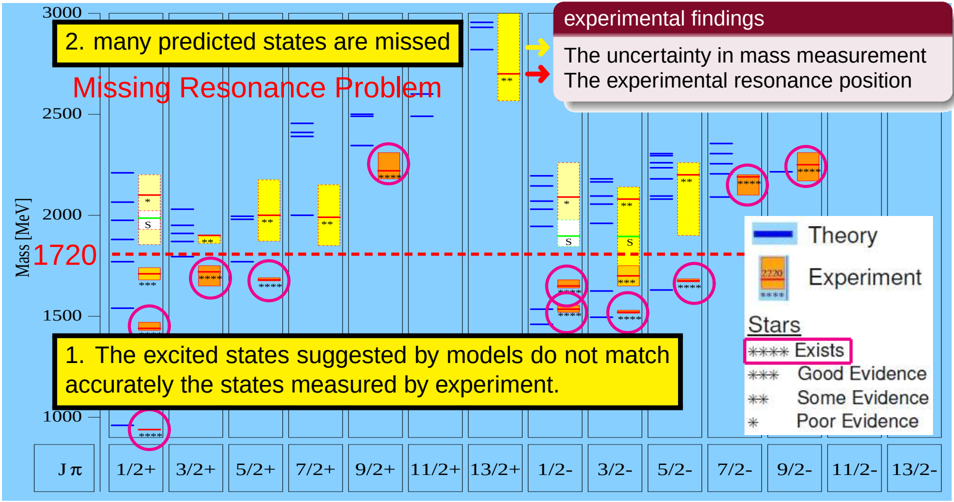

experimental findings

The uncertainty in mass measurement

The experimental resonance position

The spectrum of N^* resonances

Particle	$L_{2I \cdot 2J}$	Overall status	Status as seen in — $N\pi$	$N\eta$	ΛK	ΣK	$\Delta\pi$	$N\rho$	$N\gamma$
$N(939)$	P_{11}	****							
$N(1440)$	P_{11}	****	****	*			***	*	***
$N(1520)$	D_{13}	****	****	***			****	****	****
$N(1535)$	S_{11}	****	****	****			*	**	***
$N(1650)$	S_{11}	****	****	*	***	**	***	**	***
$N(1675)$	D_{15}	****	****	*	*		****	*	****
$N(1680)$	F_{15}	****	****	*			****	****	****
$N(1700)$	D_{13}	***	***	*	**	*	**	*	**
$N(1710)$	P_{11}	***	***	**	**	*	**	*	***
$N(1720)$	P_{13}	****	****	*	**	*	*	**	**
$N(1900)$	P_{13}	**	**					*	
$N(1990)$	F_{17}	**	**	*	*	*			*
$N(2000)$	F_{15}	**	**	*	*	*	*	**	
$N(2080)$	D_{13}	**	**	*	*				*
$N(2090)$	S_{11}	*	*						
$N(2100)$	P_{11}	*	*	*					
$N(2190)$	G_{17}	****	****	*	*	*		*	*
$N(2200)$	D_{15}	**	**	*	*				
$N(2220)$	H_{19}	****	****	*					
$N(2250)$	G_{19}	****	****	*					
$N(2600)$	$I_{1\,11}$	***	***						
$N(2700)$	$K_{1\,13}$	**	**						

The status of the N resonances

1. Nearly all existing data result from $N\pi$ channel.
   - If the missing resonances did not couple to $N\pi$, they would not have been discovered.
2. Photoproduction data accumulated mainly cover masses up to 1.7 GeV.
3. Missing resonances problem appears above 1.7 GeV.
4. The CLAS-FROST data used in this analysis covers the region above W ∼1.7 GeV.

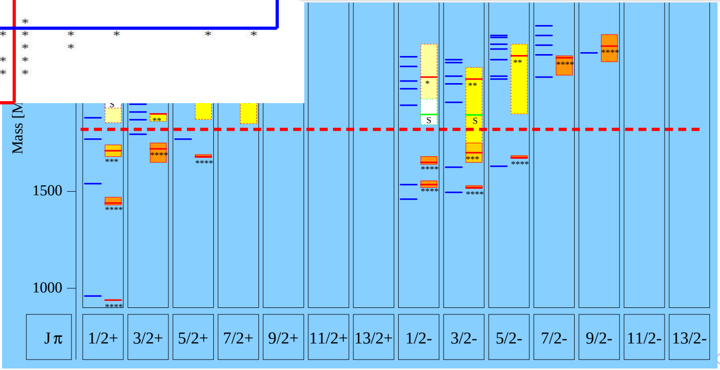

Why is $\pi^+\pi^-$ photoproduction needed ?

Particle	$L_{2I \cdot 2J}$	Overall status	Status as seen in — $N\pi$	$N\eta$	ΛK	ΣK	$\Delta\pi$	$N\rho$	$N\gamma$
$N(939)$	P_{11}	****							
$N(1440)$	P_{11}	****	****	*			***	*	***
$N(1520)$	D_{13}	****	****	***			****	****	****
$N(1535)$	S_{11}	****	****	****			*	**	***
$N(1650)$	S_{11}	****	****	*	***	**	***	**	***
$N(1675)$	D_{15}	****	****	*	*		****	*	****
$N(1680)$	F_{15}	****	****	*			****	****	****
$N(1700)$	D_{13}	***	***	*	**	*	**	*	**
$N(1710)$	P_{11}	***	***	**	**	*	**	*	***
$N(1720)$	P_{13}	****	****	*	**	*	*	**	**
$N(1900)$	P_{13}	**	**					*	
$N(1990)$	F_{17}	**	**	*	*	*			*
$N(2000)$	F_{15}	**	**	*	*	*	*	**	
$N(2080)$	D_{13}	**	**	*	*				*
$N(2090)$	S_{11}	*	*						
$N(2100)$	P_{11}	*	*	*					
$N(2190)$	G_{17}	****	****	*	*	*		*	*
$N(2200)$	D_{15}	**	**	*	*				
$N(2220)$	H_{19}	****	****	*					
$N(2250)$	G_{19}	****	****	*					
$N(2600)$	$I_{1\,11}$	***	***						
$N(2700)$	$K_{1\,13}$	**	**						

The status of the N resonances

1. Nearly all existing data result from $N\pi$ channel.
   - ◇ If the missing resonances did not couple to $N\pi$, they would not have been discovered.
2. Photoproduction data accumulated mainly cover masses up to 1.7 GeV.
3. Missing resonances problem appears above 1.7 GeV.
4. The CLAS-FROST data used in this analysis covers the region above $W \sim$1.7 GeV.

- ◇ The decay channel of $\pi^+\pi^-$ photoproduction :

  - $\gamma p \rightarrow N^* \rightarrow \Delta^{++}\pi^- \rightarrow p\pi^+\pi^-$
  - $\rightarrow \Delta^0\pi^+$
  - $\rightarrow p\rho$

- ◇ The biggest cross section contribution is from $\pi^+\pi^-$ photoproduction above W $\sim$ 1.7 GeV.

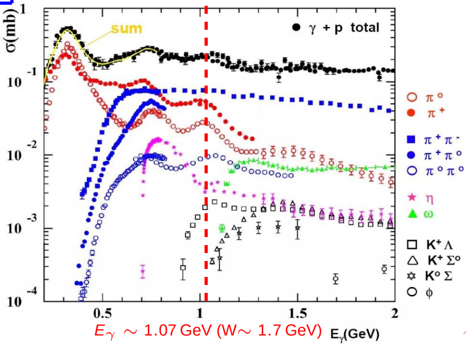

Why is $\pi^+\pi^-$ photoproduction needed ?

Particle	$L_{2I\cdot 2J}$	Overall status	Status as seen in — $N\pi$	$N\eta$	ΛK	ΣK	$\Delta\pi$	$N\rho$	$N\gamma$
$N(939)$	P_{11}	****							
$N(1440)$	P_{11}	****	****	*			***	*	***
$N(1520)$	D_{13}	****	****	***			****	****	****
$N(1535)$	S_{11}	****	****	****			*	**	***
$N(1650)$	S_{11}	****	****	*	***	**	***	**	***
$N(1675)$	D_{15}	****	****	*	*		****	*	****
$N(1680)$	F_{15}	****	****	*			****	****	****
$N(1700)$	D_{13}	***	***	*	**	*	**	*	**
$N(1710)$	P_{11}	***	***	**	**	*	**	*	***
$N(1720)$	P_{13}	****	****	*	**	*	*	**	**
$N(1900)$	P_{13}	**	**					*	
$N(1990)$	F_{17}	**	**	*	*	*			*
$N(2000)$	F_{15}	**	**	*	*	*	*	**	
$N(2080)$	D_{13}	**	**	*	*				*
$N(2090)$	S_{11}	*	*						
$N(2100)$	P_{11}	*	*	*					
$N(2190)$	G_{17}	****	****	*	*	*		*	*
$N(2200)$	D_{15}	**	**	*	*				
$N(2220)$	H_{19}	****	****	*					
$N(2250)$	G_{19}	****	****	*					
$N(2600)$	$I_{1\,11}$	***	***						
$N(2700)$	$K_{1\,13}$	**	**						

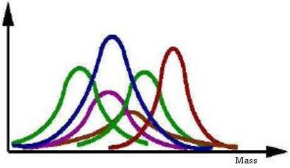

Polarization observables

- The excited states are found as broadly overlapping resonances.
- The polarization observables can isolate single resonances from other interference terms.
  - polarization observables are very sensitive to small resonant contributions.

Outline

Jefferson Laboratory in Newport News, VA

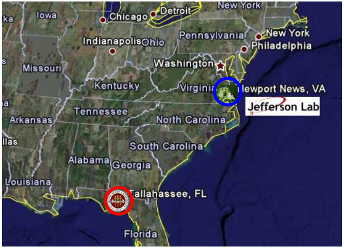

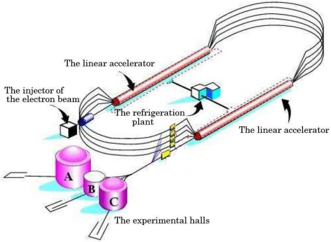

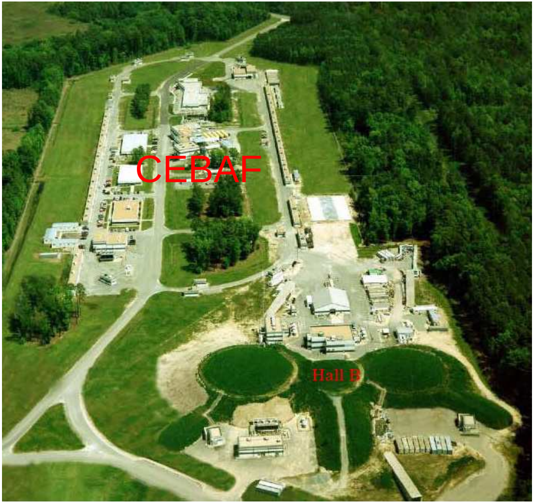

- The continuous electron beam accelerator facility (CEBAF) can deliver a continuous electron beam up to 6 GeV.

Experimental devices for the FROST experiment

- The broad-range photon tagging system
- The FROzen Spin Target (FROST)
- The CEBAF Large Acceptance Spectrometer (CLAS)

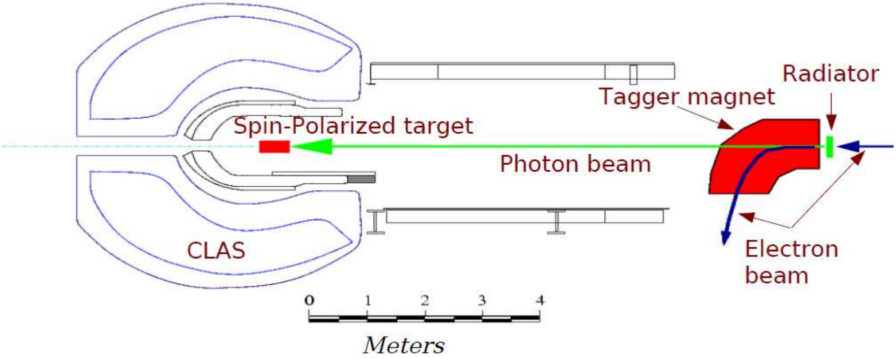

The tagging system in Hall B

JLAB Hall B bremsstrahlung photon tagger

- E_γ = 20-95 % of E_0
- E_γ up to ~5.5 GeV

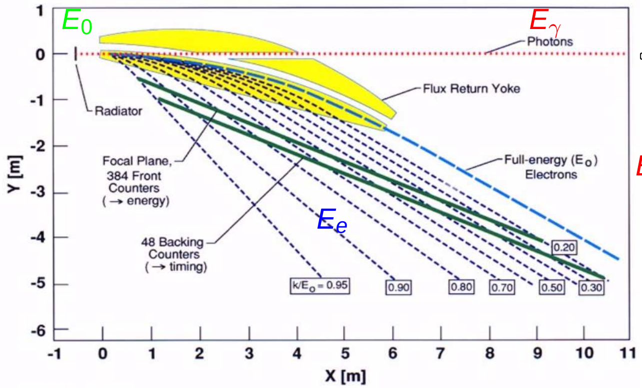

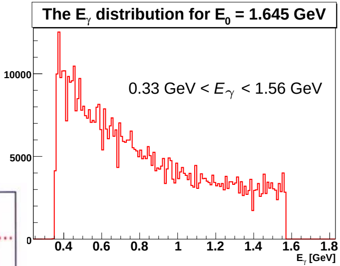

$$E_\gamma = E_0 - E_e$$

E_γ: The energy of the emitted photon

E_0: The energy of the incident electron

E_e: the energy of the outgoing electron

The tagging system in Hall B

JLAB Hall B bremsstrahlung photon tagger

- Circularly polarized photon beam — amorphous radiator — longitudinally polarized electron beam
- Linearly polarized photon beam — oriented diamod radiator — unpolarized electron beam

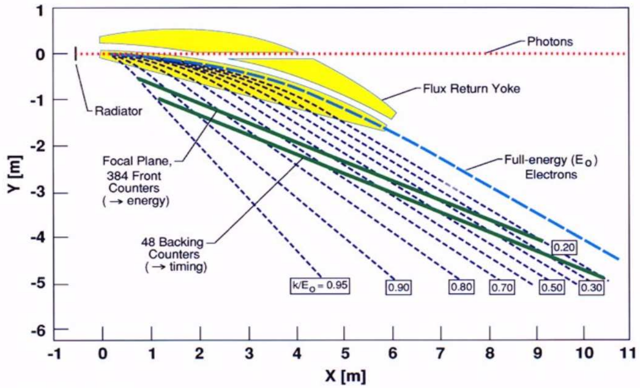

linearly polarized beam

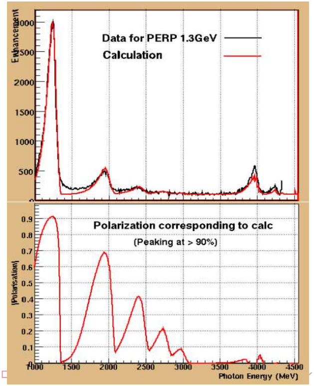

CEBAF Large Acceptance Spectrometer (CLAS)

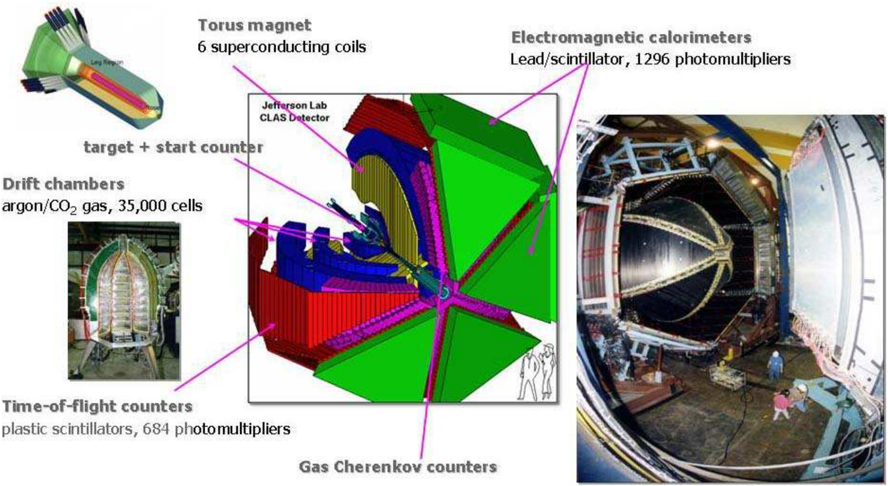

The FROzen-Spin Target (FROST)

1 High magnetic field (5 T)

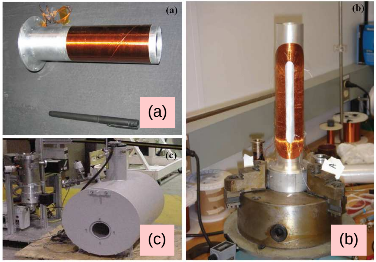

(a) The longitudinal holding magnet. (0.56 T)
(g9a : Nov. 2007 - Feb. 2008)
◇ Average target polarization
$\sim$ 82 % (+Pol) and 85 % (-Pol)

(b) The transversal holding magnet. (0.50 T)
(g9b : March 2010 - August 2010)

(c) The polarizing magnet. (5 T)

2 Low temperature

28 mK (w/o beam) and 30mK (w/ beam)

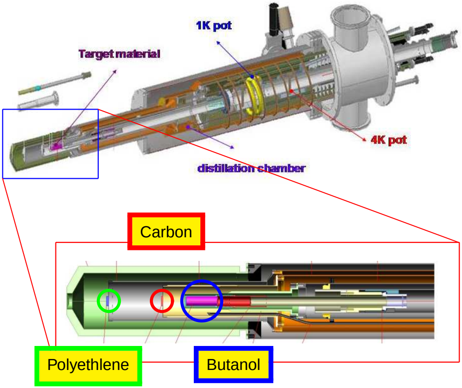

Outline

Photoproduction of $\pi^+\pi^-$ off the proton: Kinematics

- The $\pi^+ \pi^-$ photoproduction requires 5 independent variables.

ex: $E_\gamma, \theta_{\text{c.m.}}, \phi_{\pi^+}, \theta_{\pi^+}, M_{\pi^+\pi^-}$

- Other variables are integrated over in this presentation.

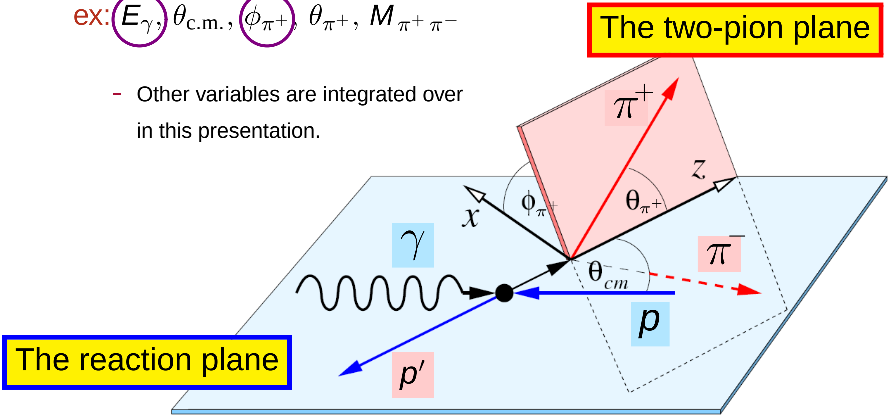

The differential cross section for $\gamma p \to p\pi^+\pi^-$

The differential cross section for $\gamma p \to p\pi^+\pi^-$

(without measuring the polarization of the recoiling nucleon)

$$\frac{d\sigma}{d x_i} = \sigma_0 \{ (1 + \vec{\Lambda}_i \cdot \vec{\mathbf{P}}) + \delta_\odot (\mathbf{I}^\odot + \vec{\Lambda}_i \cdot \vec{\mathbf{P}}^\odot)$$

$$+ \delta_l [\sin 2\beta (\mathbf{I}^\mathbf{s} + \vec{\Lambda}_i \cdot \vec{\mathbf{P}}^\mathbf{s}) + \cos 2\beta (\mathbf{I}^\mathbf{c} + \vec{\Lambda}_i \cdot \vec{\mathbf{P}}^\mathbf{c})] \}$$

- σ_0: The unpolarized cross section
- β: The angle between the direction of polarization and the x-axis
- x_i: The kinematic variables
- $\delta_{\odot,l}$: The degree of polarizaton of the photon beam $\Rightarrow \delta_\odot$, and δ_l
- $\vec{\Lambda}_i$: The polarization of the initial nucleon $\Rightarrow (\Lambda_x, \Lambda_y, \Lambda_z)$
- $\mathbf{I}^{\odot,\mathbf{s},\mathbf{c}}$: The observable arising from use of polarized photons $\Rightarrow \mathbf{I}^\odot, \mathbf{I}^\mathbf{s}, \mathbf{I}^\mathbf{c}$
- $\vec{\mathbf{P}}$: The polarization observable $\Rightarrow (\mathbf{P_x}, \mathbf{P_y}, \mathbf{P_z})$ $(\mathbf{P}_x^\odot, \mathbf{P}_y^\odot, \mathbf{P}_z^\odot)$ $(\mathbf{P}_x^s, \mathbf{P}_y^s, \mathbf{P}_z^s)$ $(\mathbf{P_x^c}, \mathbf{P_y^c}, \mathbf{P_z^c})$

15 Observables

Previous measurements

The data used for this analysis :

1. circularly-polarized beam
2. longitudinally-polarized target

$$\frac{d\sigma}{d x_i} = \sigma_0 \{ (1 + \Lambda_z \cdot \mathbf{P_z}) + \delta_\odot (\mathbf{I}^\odot + \Lambda_z \cdot \mathbf{P}_z^\odot) \}$$

$\mathbf{I}^\odot$: Phys.Rev.Lett. 95, 162003 (2005, CLAS Collaboration)

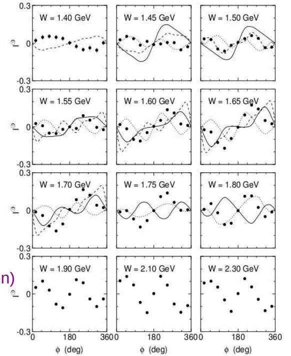

$\mathbf{I}^\odot$: Phys.Rev.Lett. 103, 052002

(2009, Crystal Ball at MAMI, TAPS, and A2 Collaboration)

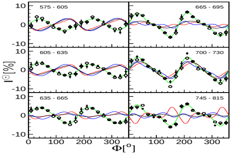

$\mathbf{P}_z^\odot$: Eur.Phys.J. A 34, 11-21 (2007, GDH Collaboration)

- The helicity-dependent total cross-section difference

$$\Delta\sigma = (\sigma_{3/2} - \sigma_{1/2})$$

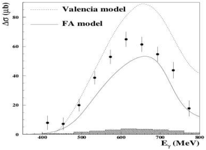

Basic event selection

photon selection

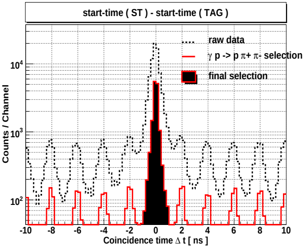

proton and pion selection

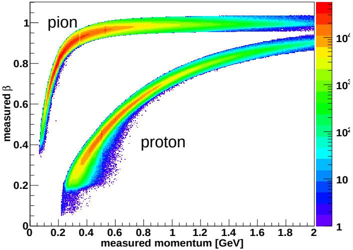

vertex cut

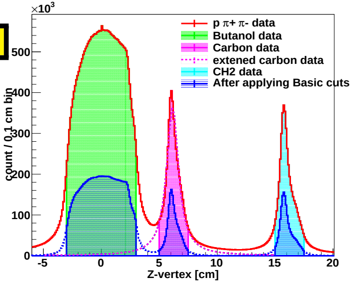

- Basic Cuts
  - photon selection
    : $|\ \Delta t\ | < 1.2$ ns
  - proton selection
    : $|\ \Delta\beta\ | < 0.032$
  - pion selection
    : $|\ \Delta\beta\ | < 0.044$
  - vertex cut (Butanol)
    : $|\ Zvertex\ | < 3$ cm
  - accidental cut
    : one photon selection
  - confidence-level cut
    : CL-cut > 5 %

Basic event selection

- The kinematic fitting

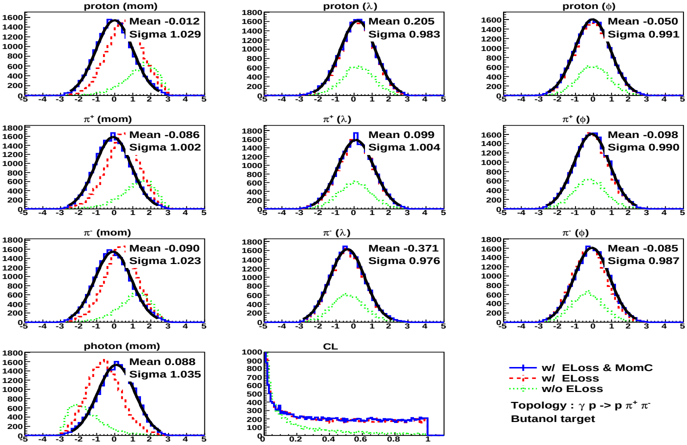

- Basic Cuts
  - photon selection
    - : $|\ \Delta t\ | < 1.2$ ns
  - proton selection
    - : $|\ \Delta\beta\ | < 0.032$
  - pion selection
    - : $|\ \Delta\beta\ | < 0.044$
  - vertex cut (Butanol)
    - : $|\ Zvertex\ | < 3$ cm
  - accidental cut
    - : one photon selection
  - confidence-level cut
    - : CL-cut > 5 %
- Corrections
  - Energy-loss correction
  - Photon-energy correction
  - Momentum correction

Outline

Polarization observable **I** $^{\odot}$

Polarization observable $\mathbf{I}^{\odot}$

$$\mathbf{I}^{\odot}(\mathbf{W},\ \phi_{\pi^+}) = \frac{1}{\bar{\delta}_{\odot}(\mathbf{W})} \frac{\left\{ N(\rightarrow; \mathbf{W}, \phi_{\pi^+})_{beam} - N(\leftarrow; \mathbf{W}, \phi_{\pi^+})_{beam} \right\}}{\left\{ N(\rightarrow; \mathbf{W}, \phi_{\pi^+})_{beam} + N(\leftarrow; \mathbf{W}, \phi_{\pi^+})_{beam} \right\}}$$

- $\bar{\delta}_{\odot}(\mathbf{W})$: The average degree of the photon beam polarizations.
- $\rightarrow (\leftarrow)$: the direction of the beam polarization is parallel (anti-parallel) to the beam.
- Beam-helicity asymmetry for the unpolarized target and circularly-polarized photon beam.

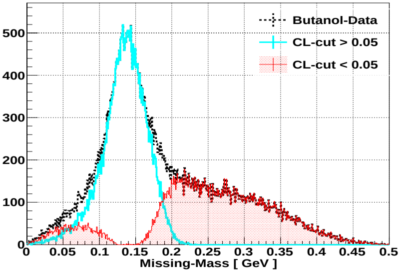

example :

- Topology : $\gamma p \rightarrow p\pi^{+}(\pi^{-})$.
- W : 1.60 GeV.
- $\theta_{\text{c.m.}},\ \phi_{\pi^+},\ \theta_{\pi^+},\ M_{\pi^+\pi^-}$ are integrated over.
- Using the 5 % Confidence Level Cut
  - There is still an effect of background events.

The background effect in Beam-Helicity Asymmetry $I^{\odot}$

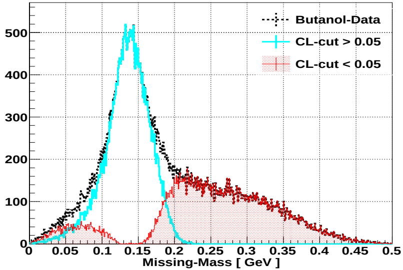

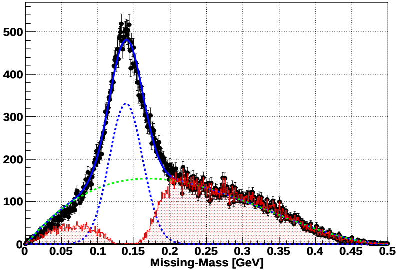

- Fitting function : Gaussian + Chebyshev pol.

- Butanol data are composed of
  - free-proton data
  - bound-nucleon data & background data
- After applying CL-cut, there are still bound-nucleon and background events.
- These bound-nucleon and background events have a small influence on the beam asymmetry.

Check the symmetry of polarization observable $I^{\odot}$

- Kinematic variables $\theta_{\mathrm{c.m.}}, \theta_{\pi^+}, M_{\pi^+\pi^-}$ are integrated over.
- Butanol$(2\pi - \phi)$: $-I^{\odot}(2\pi - \phi)$

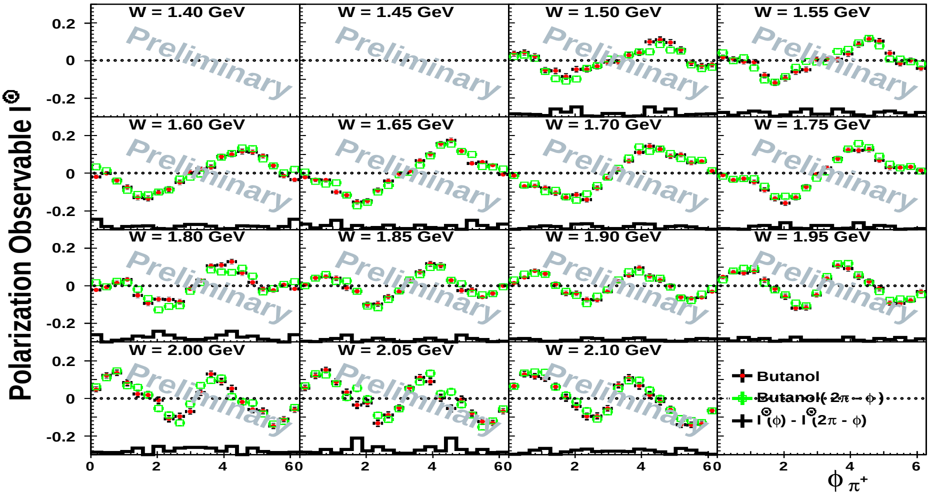

Beam-Helicity Asymmetry I$^{\odot}$ with the published data

- I$^{\odot}$: Phys.Rev.Lett. 95, 162003 (2005, CLAS Collaboration)

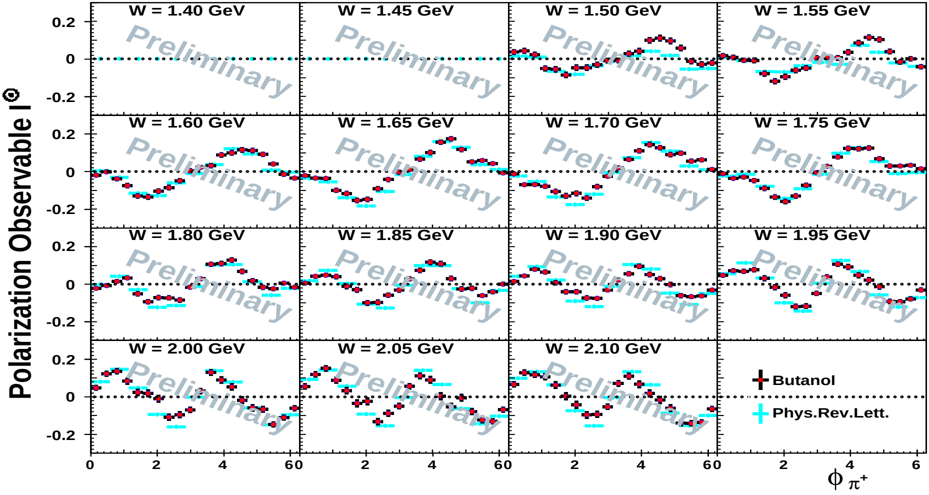

Q-factor method

- The Q-factor method is used to subtract background :
  - The Q-factor is an event-based quality factor which denotes the probability that each seed event is a signal event.

- Find the input for the Q-factor method :
  - Step 1) The 300 nearest neighbors from the butanol seed event are selected. (in black)
  - Step 2) A seed event in the carbon sample is chosen which is kinematically closest to the butanol seed event.
  - Step 3) The 300 nearest neighbors for the carbon seed event are selected. (in green)

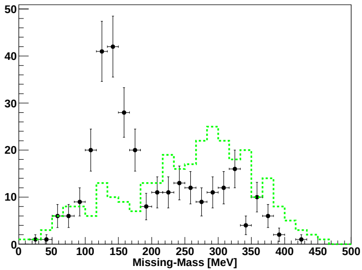

- The distance between event a and b, $D^2_{a,b}$:

$$D^2_{a,b} = \sum_{i=1}^{4} \left(\frac{\Gamma_i^a - \Gamma_i^b}{\Delta_i} \right)^2$$

Γ_i : $W, \theta^{proton}_{\mathrm{c.m.}}, \phi_{\pi^+}, \theta_{\pi^+}$

Δ_i : the maximum range of the kinematic variable Γ_i

Q-factor method

For each event,

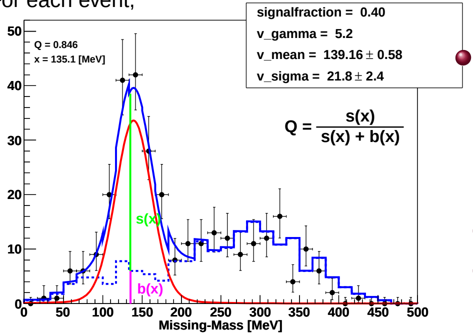

- The Q-factor is:

$$Q = \frac{s(x)}{s(x) + b(x)}$$

1. x : the missing mass of the seed event
2. $s(x)$: $f_s \cdot S(x)$
3. $b(x)$: $(1 - f_s) \cdot B(x)$

- The total function (in blue) is:

$$f(x) = N \cdot [f_s \cdot S(x) - (1 - f_s) \cdot B(x)]$$

➜ There are four parameters decided.

1. $S(x)$: the Voigt function (Γ, *mean*, and σ)
2. $B(x)$: the background function
   - g9b carbon distribution (in green)
3. N : a normalization constant
4. f_s : the signal fraction with [0,1]

➜ event-based scale factor, **s** is the parameter to scale the carbon distribution.

$$\mathbf{s} = \frac{(1-f_s)\cdot(\#\text{ of nearest butanol events})}{(\#\text{ of nearest carbon events})} = 1 - f_s$$

Q-factor method

- The order to decide four parameters is:

Step1 Variables for the Voigt function are decided.

- *mean* : [139, 140] MeV
- σ : [5, 200] MeV
- Γ : the small fixed value from a similar fit to the fully integrated distribution.

Step2 event-based scale factor, s (= 1 - f_s) are decided by the following two plots:

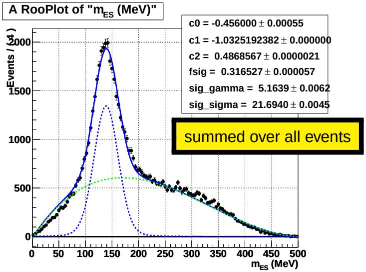

general-method / Q-factor

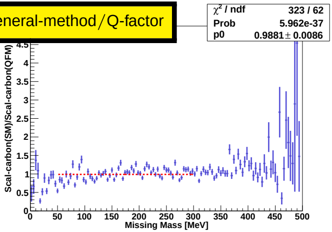

χ^2 distribution

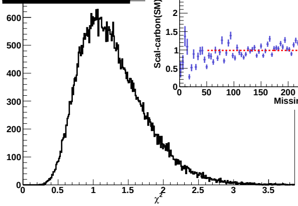

Topology: $\gamma p \to p\pi^+(\pi^-)$ and W: 1.6 GeV

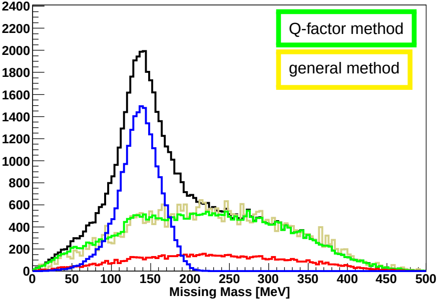

Q-factor method

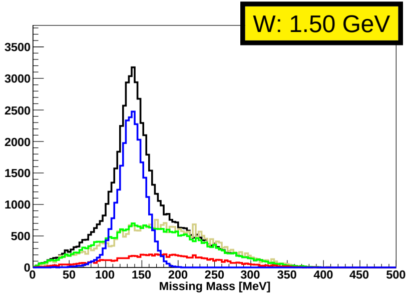

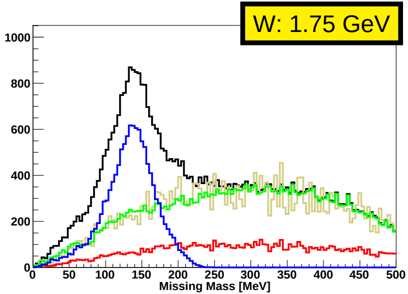

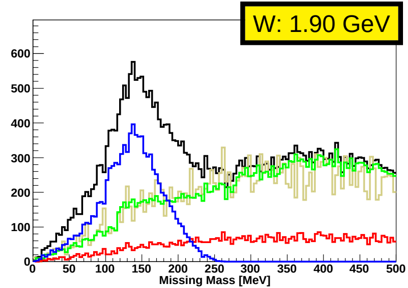

- Topology: $\gamma p \rightarrow p\pi^{+}(\pi^{-})$.
- The Q-factor method is used as an event-based dilution factor to subtract background.
- From the butanol (C_4H_9OH) data, the free proton data is extracted on an event-by-event basis. No overall dilution factor is necessary.

Beam-Helicity Asymmetry $I^{\odot}$ with models

- FSU-model calculated by Winston Roberts
- A.Fix-model calculated by Alexander Fix (Eur. Phys. J. A 25, 115-135, 2005)

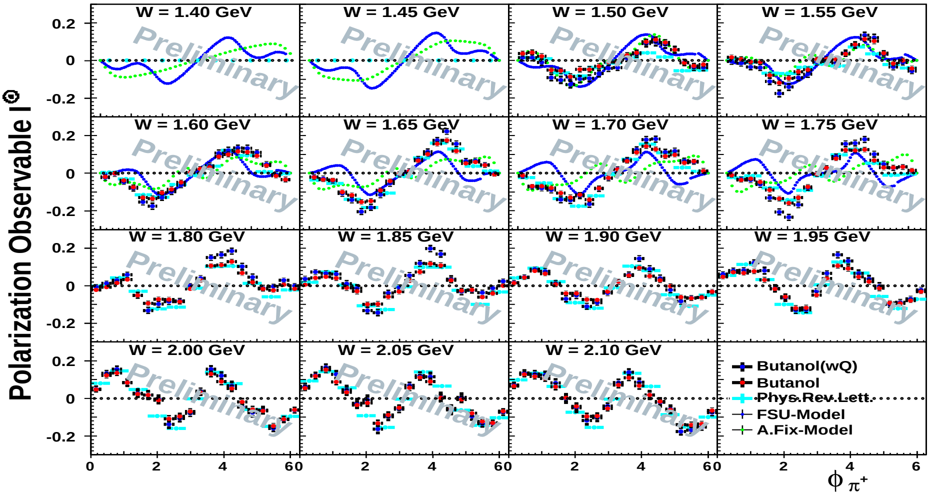

Polarization observable $\mathbf{P_z}$

Polarization observable $\mathbf{P_z}$

$$\mathbf{P_z}(\mathbf{W}, \phi_{\pi^+}) = \frac{1}{\overline{\Lambda}_z(\mathbf{W})} \frac{\left\{ N(\Rightarrow; \mathbf{W}, \phi_{\pi^+})_{target} - N(\Leftarrow; \mathbf{W}, \phi_{\pi^+})_{target} \right\}}{\left\{ N(\Rightarrow; \mathbf{W}, \phi_{\pi^+})_{target} + N(\Leftarrow; \mathbf{W}, \phi_{\pi^+})_{target} \right\}}$$

- $\overline{\Lambda}_z(\mathbf{W})$: The average degree of the target polarizations.
- $\Rightarrow$ ($\Leftarrow$) : the direction of the target polarization is parallel (anti-parallel) to the beam.
- Target asymmetry for the linearly-polarized target and unpolarized photon beam.

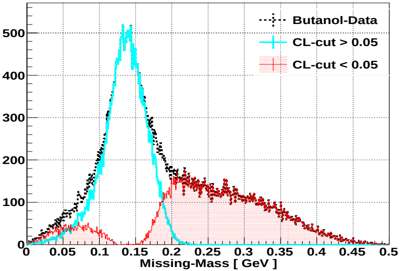

example :

- Topology : $\gamma p \to p\pi^+(\pi^-)$.
- W : 1.60 GeV.
- $\theta_{\mathrm{c.m.}}, \phi_{\pi^+}, \theta_{\pi^+}, M_{\pi^+\pi^-}$ are integrated over.
- Using the 5 % Confidence Level Cut & Q-factor method

Check the symmetry of polarization observable P_z

- Kinematic variables $\theta_{\mathrm{c.m.}}, \theta_{\pi^+}, M_{\pi^+\pi^-}$ are integrated over.
- Butanol(wQ)($2\pi - \phi$) : $-P_z(2\pi - \phi)$

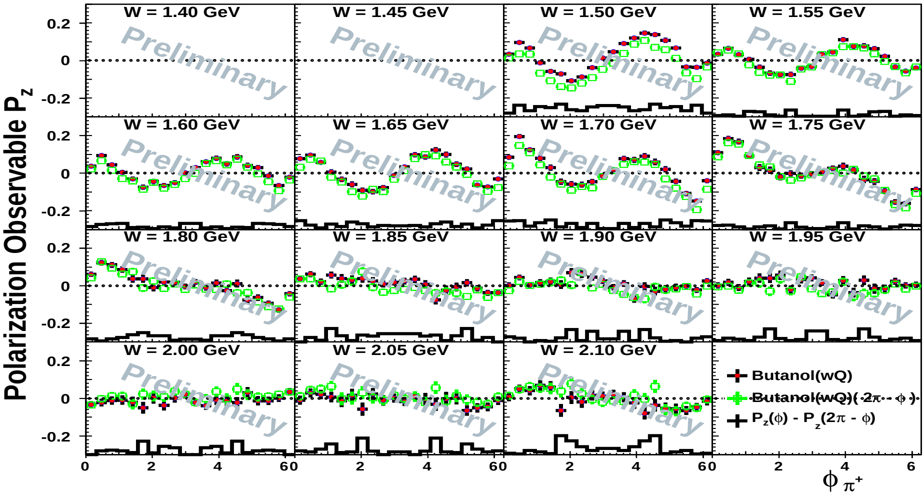

Target Asymmetry P_z with models

- FSU-model calculated by Winston Roberts
- A.Fix-model calculated by Alexander Fix (Eur. Phys. J. A 25, 115-135, 2005)

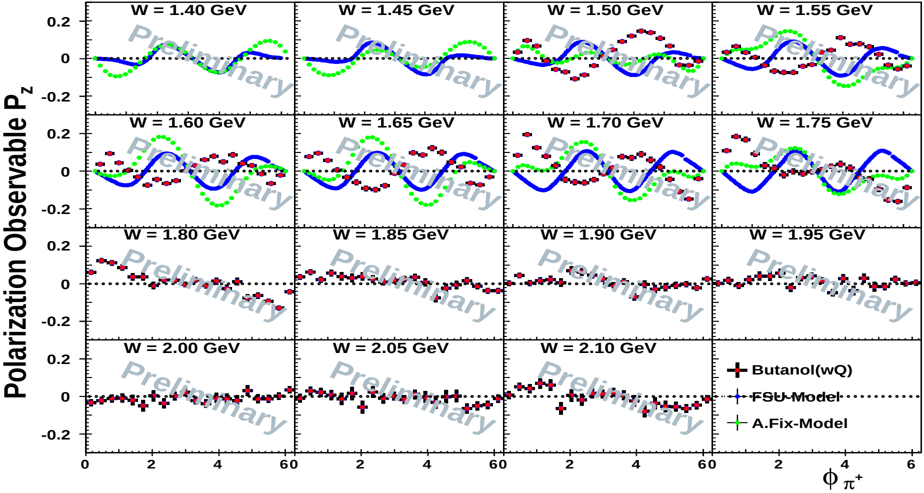

Polarization observable $\mathbf{P_z^{\odot}}$

Polarization observable $P_z^{\odot}$

$$P_z^{\odot}(\mathbf{W}, \phi_{\pi^+}) = \frac{1}{\bar{\Lambda}_z(\mathbf{W}) \cdot \bar{\delta}_{\odot}} \frac{\left\{ N(\mathbf{W}, \phi_{\pi^+})_{3/2} - N(\mathbf{W}, \phi_{\pi^+})_{1/2} \right\}}{\left\{ N(\mathbf{W}, \phi_{\pi^+})_{3/2} + N(\mathbf{W}, \phi_{\pi^+})_{1/2} \right\}}$$

- ◇ $\bar{\Lambda}_z(\mathbf{W})$: The average degree of the target polarizations.
- ◇ $\bar{\delta}_{\odot}(\mathbf{W})$: The average degree of the photon beam polarizations.
- ◇ Helicity Difference for the linearly-polarized target and circularly-polarized photon beam.

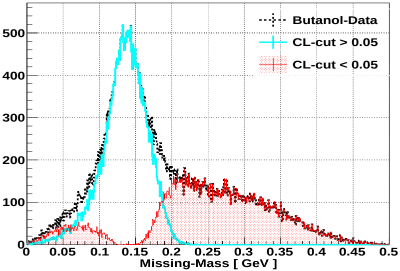

example :

- Topology : $\gamma p \to p\pi^+(\pi^-)$.
- W : 1.60 GeV.
- $\theta_{\text{c.m.}}, \phi_{\pi^+}, \theta_{\pi^+}, M_{\pi^+\pi^-}$ are integrated over.
- Using the 5 % Confidence Level Cut & Q-factor method

Check the symmetry of polarization observable $P_z^{\odot}$

- Kinematic variables $\theta_{\text{c.m.}}$, θ_{π^+}, $M_{\pi^+\pi^-}$ are integrated over.
- Butanol(wQ)($2\pi - \phi$) : $P_z^{\odot}(2\pi - \phi)$

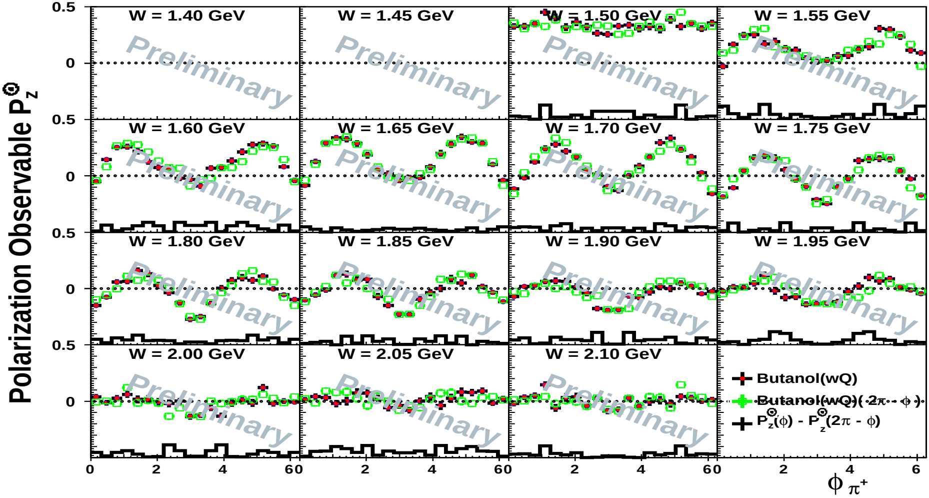

Helicity Difference $P_z^{\odot}$

- FSU-model calculated by Winston Roberts
- A.Fix-model calculated by Alexander Fix (Eur. Phys. J. A 25, 115-135, 2005)

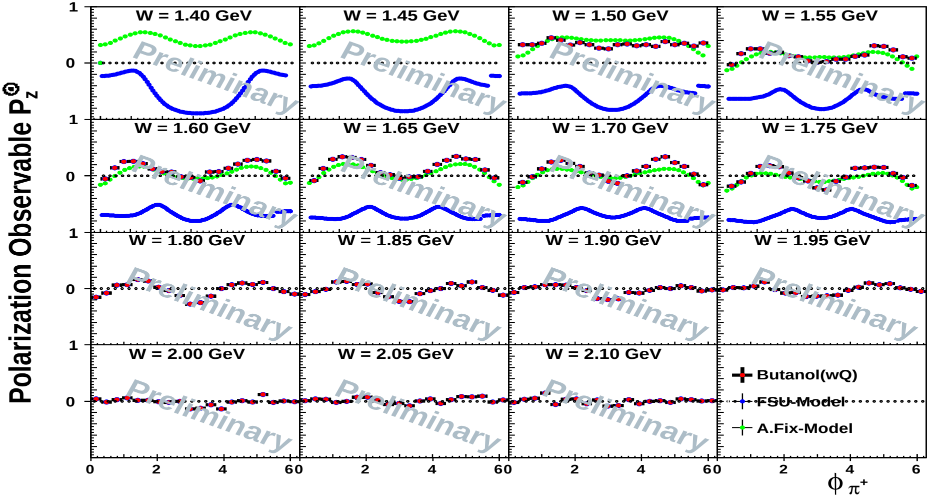

Outline

Summary

- Polarization Observable $\mathbf{I}^{\odot}$ using the FROST data is in good agreement with the previously published CLAS data.
- Polarization Observables $\mathbf{P_z}$ and $\mathbf{P_z^{\odot}}$ will be first-time measurements for double-pion photoproduction.
- The comparison between results from the butanol target and the butanol weighted by the Q-factor (event-based background subtraction) shows that the Q-factor method is very useful tool to extract the polarization observables.
- The comparison with model predictions provides the basis for significant improvements for the models.

Korea Multi-Purpose Accelerator Complex

Korea Multi-Purpose Accelerator Complex

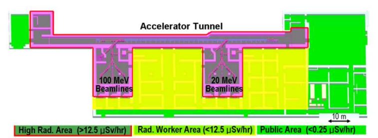

❖ **User Program Development (2003~)**

Research Fields	Sub-categories
Nano Science & Technology	Ion-cutting, Nano-particle shaping & fabrication, Carbon nano-tube, nano-wire, Nano-machining
Information Technology	High power semiconductor, Semiconductor manufacturing R&D, Proton lithography
Space Technology	Radiation hard electronic device, Radiation effect on materials
Bio-Technology	Mutation of plants & micro-organisms
Medical research	Low energy proton therapy study, Biocompatible material, Biological radiation effects, New RI production R&D
Materials Science	Proton irradiation effects with various materials Gemstone coloration
Energy & Environment	New microorganism development for bio fuel (ethanol, butanol), New materials for fuel cell ; electrolyte, nano catalyst, organic solar cell
Nuclear & Particle Physics	Detector R&D, Nuclear data, TLA (Thin Layer Activation)

Back up

Quark

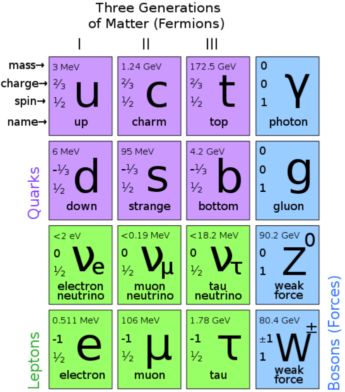

- electric charge **Q** : $\mathbf{I_z} + \frac{\beta + \mathbf{S} + \mathbf{C} + \mathbf{B} + \mathbf{T}}{2}$
  ex:
  - $\mathbf{Q}(u) = \frac{1}{2} + \frac{1/3+0+0+0+0}{2} = +\frac{2}{3}$
  - $\mathbf{Q}(d) = -\frac{1}{2} + \frac{1/3+0+0+0+0}{2} = -\frac{1}{3}$
  - $\mathbf{Q}(s) = 0 + \frac{1/3-1+0+0+0}{2} = -\frac{1}{3}$
  - $\mathbf{Q}(c) = 0 + \frac{1/3+0+1+0+0}{2} = +\frac{2}{3}$
  - $\mathbf{Q}(b) = 0 + \frac{1/3+0+0-1+0}{2} = -\frac{1}{3}$
  - $\mathbf{Q}(t) = 0 + \frac{1/3+0+0+0+1}{2} = +\frac{2}{3}$

	d	u	s	c	b	t
J - total angular momentum	+1/2	+1/2	+1/2	+1/2	+1/2	+1/2
Q - electric charge	-1/3	+2/3	-1/3	+2/3	-1/3	+2/3
I - isospin	1/2	1/2	0	0	0	0
$\mathbf{I_z}$ - isospin z-component	-1/2	+1/2	0	0	0	0
β - baryon number	+1/3	+1/3	+1/3	+1/3	+1/3	+1/3
S - strangeness	0	0	-1	0	0	0
C - charm	0	0	0	+1	0	0
B - bottomness	0	0	0	0	-1	0
T - topness	0	0	0	0	0	+1

Hadron : SU(3)

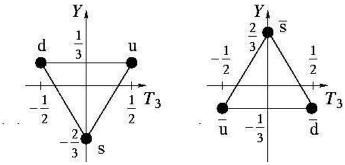

- **Y** : the hypercharge = β(baryon number) + **S**(strangeness)
- **T**$_3$: the isospin z-component
- Young Tableaux for SU(n) : dim YT = N/D

Meson octet singlet

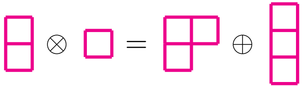

$$\bar{3} \otimes 3 = 8 \oplus 1$$

Baryon decuplet octet singlet

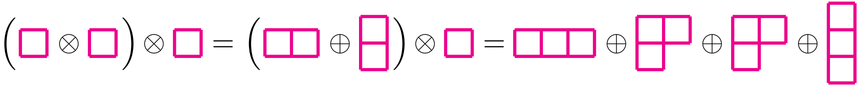

$$(3 \otimes 3) \otimes 3 = (6 \oplus 3) \otimes 3 = 10 \oplus 8 \oplus 8 \oplus 1$$

Meson

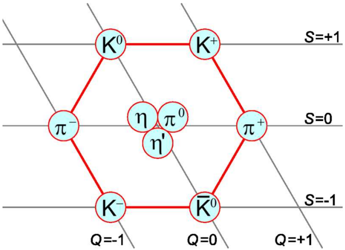

- The $J^P = 0^-$ pseudoscalar meson nonet
- $n^{2s+1} l_J \;\; J^{PC} : 1^1 S_0 \;\; 0^{-+}$
  - $n = 1$, $l = 0$, $s = 0$, and $J = 0$

I=1	I=1/2	I=0	I=0
$\pi^+ : u\bar{d}$ (**Q**=1:**S**=0)	$K^+ : u\bar{s}$ (**Q**=1:**S**=1)	η $\frac{(u\bar{u}+d\bar{d}-2s\bar{s})}{\sqrt{6}}$ (**Q**=0:**S**=0)	$\eta'(958)$ $\frac{(u\bar{u}+d\bar{d}+s\bar{s})}{\sqrt{3}}$ (**Q**=0:**S**=0)
$\pi^0 : \frac{1}{\sqrt{2}}(d\bar{d} - u\bar{u})$ (**Q**=0:**S**=0)	$K^0 : d\bar{s}$ (**Q**=0:**S**=1) $\bar{K}^0 : \bar{d}s$ (**Q**=0:**S**=-1)		
$\pi^- : \bar{u}d$ (**Q**=-1:**S**=0)	$K^- : \bar{u}s$ (**Q**=-1:**S**=-1)		

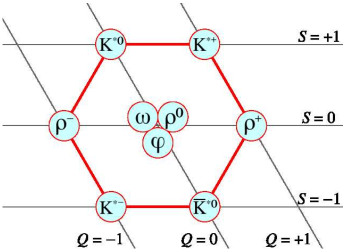

- The $J^P = 1^-$ vector meson nonet
- $n^{2s+1} l_J \;\; J^{PC} : 1^3 S_1 \;\; 1^{--}$
  - $n = 1$, $l = 0$, $s = 1$, and $J = 1$

I=1	I=1/2	I=0	I=0
$\rho^+ : u\bar{d}$ (**Q**=1:**S**=0)	$K^{*+} : u\bar{s}$ (**Q**=1:**S**=1)	$\phi(1020)$ $s\bar{s}$ (**Q**=0:**S**=0)	$\omega(782)$ $\frac{u\bar{u}+d\bar{d}}{\sqrt{2}}$ (**Q**=0:**S**=0)
$\rho^0 : \frac{1}{\sqrt{2}}(d\bar{d} - u\bar{u})$ (**Q**=0:**S**=0)	$K^{*0} : d\bar{s}$ (**Q**=0:**S**=1) $\bar{K}^{*0} : \bar{d}s$ (**Q**=0:**S**=-1)		
$\rho^- : \bar{u}d$ (**Q**=-1:**S**=0)	$K^{*-} : \bar{u}s$ (**Q**=-1:**S**=-1)		

Meson

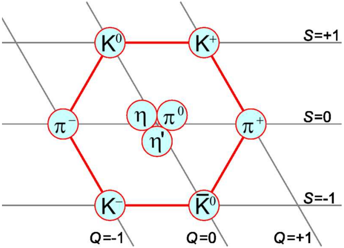

- The $J^P = 0^-$ pseudoscalar meson nonet

$\pi^{\pm}(139.5) : I^G(J^P) = 1^-(0^-)$

$\pi^0(135) : I^G(J^{PC}) = 1^-(0^{-+})$

$K^{\pm}(494) : I(J^P) = \frac{1}{2}(0^-)$

$K^0(498) : I(J^P) = \frac{1}{2}(0^-)$

$\eta(548) : I^G(J^{PC}) = 0^+(0^{-+})$

$\eta'(958) : I^G(J^{PC}) = 0^+(0^{-+})$

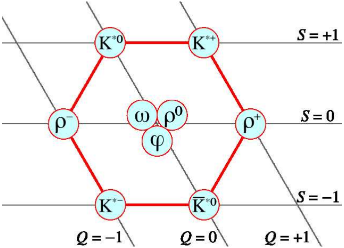

- The $J^P = 1^-$ vector meson nonet

$\rho(770) : I^G(J^P) = 1^+(1^{--})$

$K^*(892) : I(J^P) = \frac{1}{2}(1^-)$

$\omega(783) : I^G(J^{PC}) = 0^-(1^{--})$

$\phi(1020) : I^G(J^{PC}) = 0^-(1^{--})$

Baryon

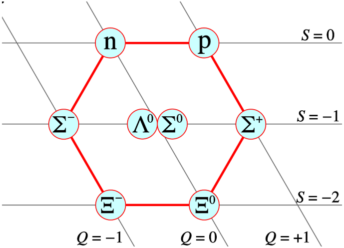

- The $J^P = \frac{1}{2}^+$ baryon octet

$p(938) : I(J^P) = \frac{1}{2}(\frac{1}{2}^+)$	$n(939) : I(J^P) = \frac{1}{2}(\frac{1}{2}^+)$
$\Sigma^+(1189) : I(J^P) = 1(\frac{1}{2}^+)$	$\Sigma^-(1197) : I(J^P) = 1(\frac{1}{2}^+)$
$\Lambda^0(1115) : I(J^P) = 0(\frac{1}{2}^+)$	$\Sigma^0(1192) : I(J^P) = 1(\frac{1}{2}^+)$
$\Xi^0(1315) : I(J^P) = \frac{1}{2}(\frac{1}{2}^+)$	$\Xi^-(1322) : I(J^P) = \frac{1}{2}(\frac{1}{2}^+)$

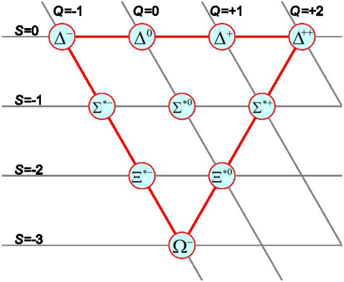

- The $J^P = \frac{3}{2}^+$ baryon decuplet

$\Delta(1232) : I(J^P) = \frac{3}{2}(\frac{3}{2}^+)$

$\Delta^*(1385) : I(J^P) = 1(\frac{3}{2}^+)$

$\Xi^*(1530) : I(J^P) = \frac{1}{2}(\frac{3}{2}^+)$

$\Omega^-(1672) : I(J^P) = 0(\frac{3}{2}^+)$

Quantum Chromodynamics (QCD)

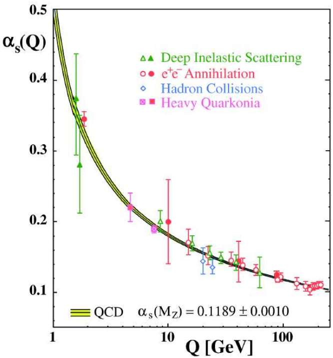

- QCD is the theory of strong interactions; the strong force describes the interactions of quarks and gluons making up hadrons.

1. Asymptotic Freedom

When the exchange momentum Q is great, quarks and gluons interact very weakly.

➜ The inside of the proton at high energies, a "dense soup" of quarks and gluons.

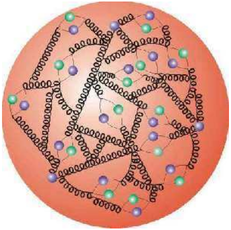

2.Confinement

Force between quarks does not diminish
as they are separated.

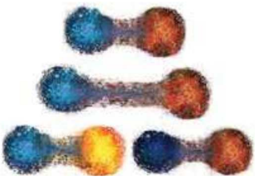

The γ-N interaction

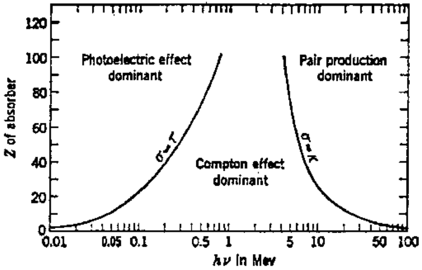

- What happen in the γ-N interaction ?
  - No interaction
  - Photoelectric effect
  - Compton scattering effect
  - Pair production effect
  - Hadronic interaction

- Photoelectric effect
  - Photon undergoes an interaction with an absorber atom in which the photon completely disappears. In this place, an energetic photoelectron is ejected
- Compton scattering effect
  - The compton effect is equivalent to inelastic collision of photon with electrons. Part of the photon energy is lost to the electron, and a less-energetic photon bounce off.
- Pair production
  - At the vicinity of an atom, a photon with energy greater than 1.02 MeV creates a positron-electron pair, and such a process is called pair production.

The spectrum of N^* resonances

(D, L_N^P)

- bands with the same number **N** of quanta of excitation.
- **D**: the dimensionality of the SU(6) representation.
- **L**: the total quark orbital angular momentum.
- **P**: the total parity

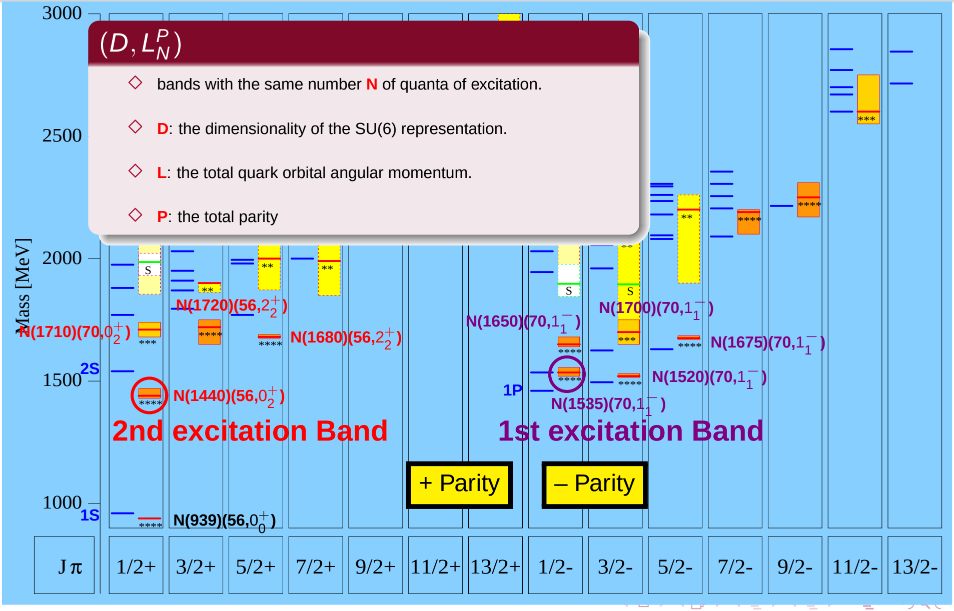

Double pion-production in the second resonance region

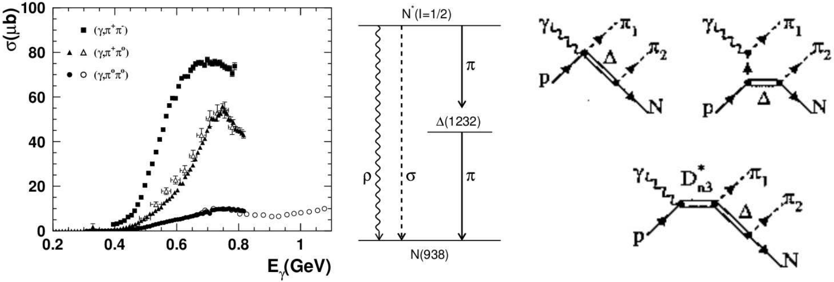

- Total cross section of the three isospin channels of double pion production on the proton.
- Possible resonance contributions to double pion production in the second resonance region.
  - N^*(I=1/2) $\to$ N(938)ρ
    $\to$ N(938)f_0(600)
    $\to$ δ(1232)π $\to$ N(938)$\pi\pi$
- An important contribution is assigned to the $\gamma p \to \Delta^{++}\pi^-$ channel while the $\gamma p \to \Delta^0\pi^+$ channel is negligible.

Calibration

- The process of the data acquisition

Step 1 A trigger is detected. (The g9a experiment has used a trigger which required at least one charged particle in CLAS spectrometer.)

Step 2 Time counters in detectors start measuring the time.

Step 3 When a signal is detected, they stop and record the data.

- The calibration of all detector components
  - The calibration aligns their timing with the beam radio frequency time (RF or accelerator time).
  - An electron beam bucket is supplied to the target about every 2 ns.

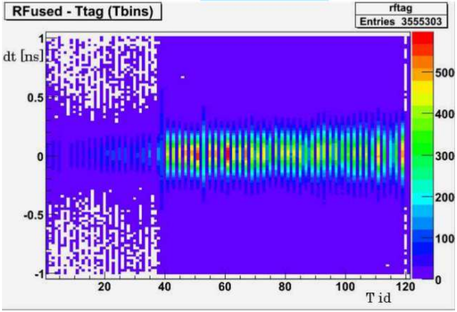

- Tagger Calibration
  - dt = (Time reconstructed in the tagger at the target center) – (RF time identified nearest bucket at the target center)
  - T counter is matched to the RF bucket

Calibration

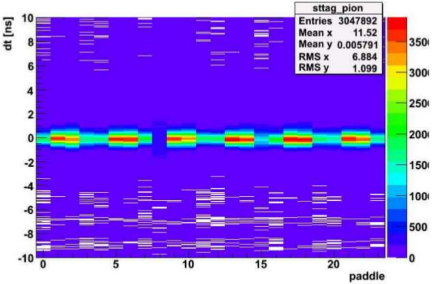

- ST Calibration
  - dt = (RF vertex time) - (ST vertex time)
  - offsets are around zero

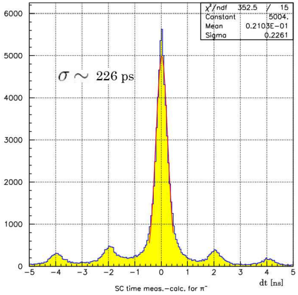

- TOF Calibration
  - dt = (RF vertex time) - (TOF vertex time)
  - The time-of-flight times are corrected for the flight time back to the target.
  - Particle identification in CLAS
    relies on the combination of measured charged-particle momenta (from DC) and the flight time from the target to the respective TOF counters.

Drift chamber(DC) Calibration

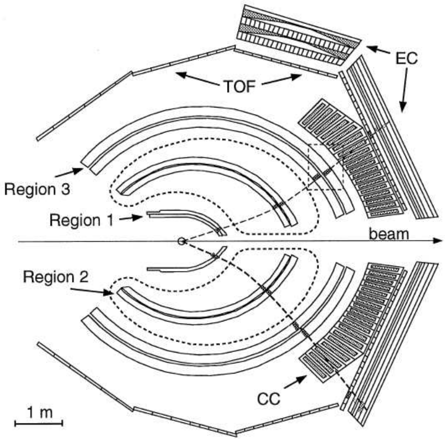

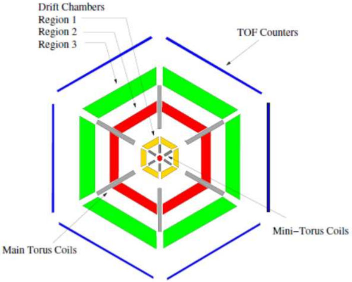

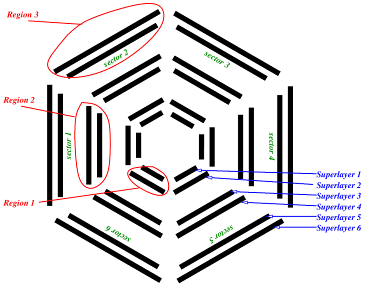

$p = qBR$

- p : the momentum
- q : the sign of the charge
- R : the radius of the curvature
- B : the magnetic field

Drift chamber(DC) Calibration

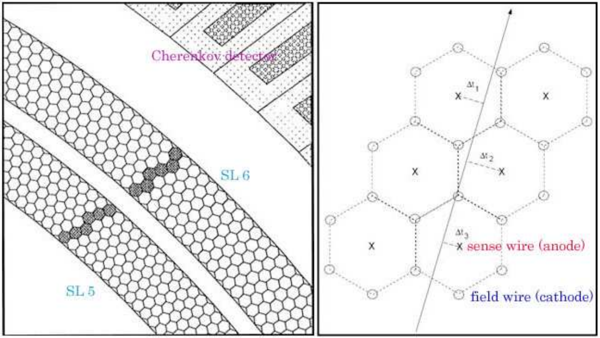

- The DC are in a magnetic field and produce the curvature of the particle.
  - Thin wires are fixed in a volume filled with the gas mixture (90% argon and 10% CO_2).
  - The DC has a quasi-hexagonal pattern as the cell form with six field wires (cathodes) surrounding one sense wire (anode)
  - A traversing charged particle ionizes the gas inside these cells and the electrons drift to the sense wire.

Drift chamber(DC) Calibration

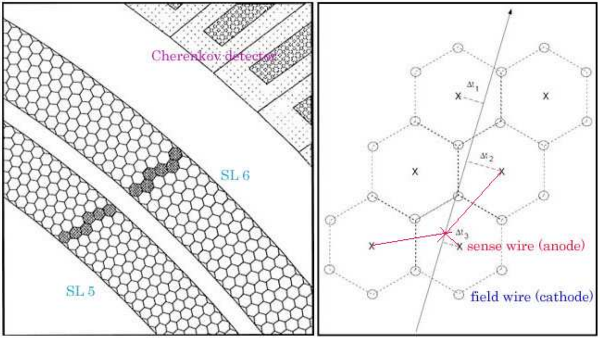

- The fitted DOCA and drift time is found.
  - DOCA means the distance of closest approach of the charged particle to the sense wire.

Drift chamber(DC) Calibration

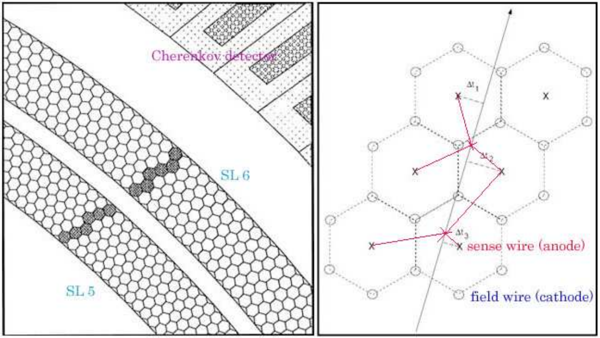

- The fitted DOCA and drift time is found.

Drift chamber(DC) Calibration

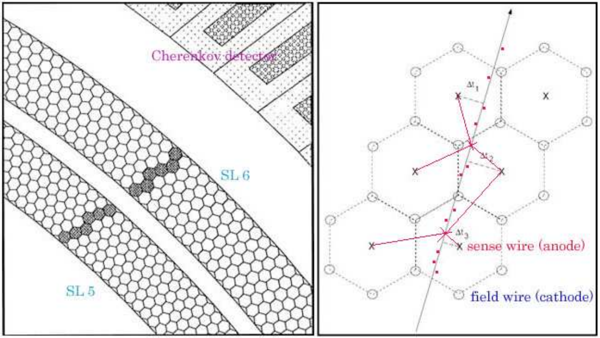

- The fitted DOCA and drift time is found.

Drift chamber(DC) Calibration

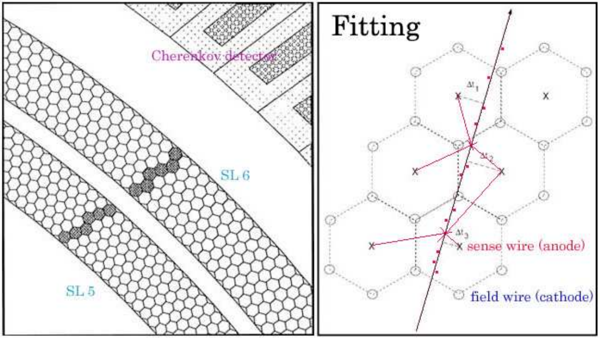

- The fitted DOCA and drift time is found.

Drift chamber(DC) Calibration

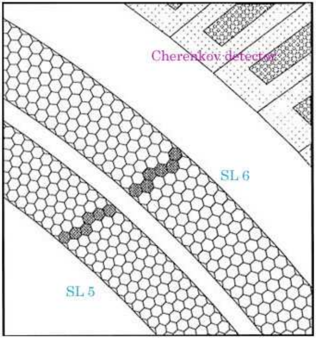

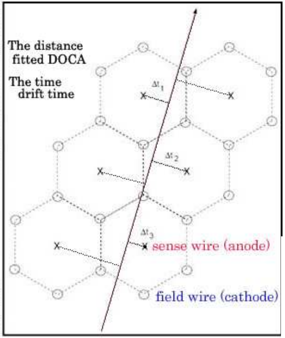

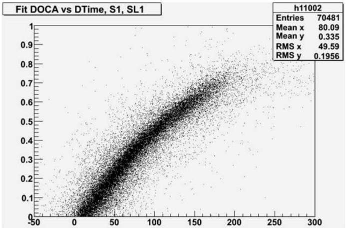

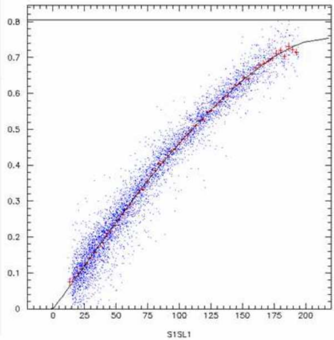

- The fitted DOCA and drift time is found.
- The drift velocity function is found using fitting.
- The calculated DOCA is found using the velocity and the drift time.

Drift chamber(DC) Calibration

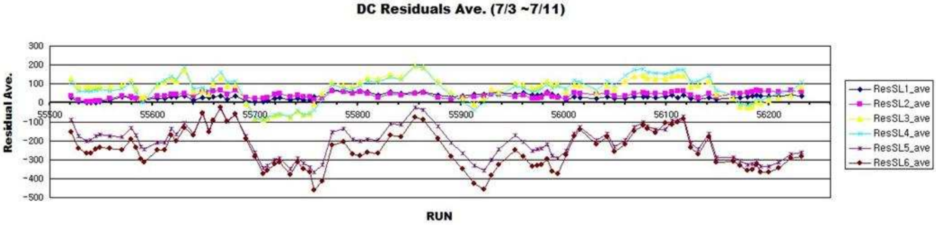

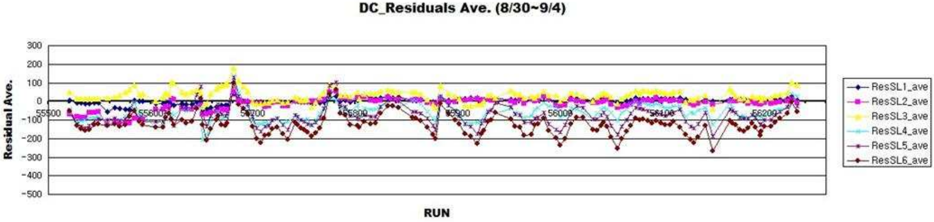

- Average DC residuals before starting (the top) and after finishing (the bottom) DC calibration in the g9a dataset.

Residual = calculated DOCA - fitted DOCA

The Frozen-Spin Target (FROST)

Operation is more complicated:

(1) Polarize target material via DNP at 5 T and 0.5 K (Polarizing Mode)

(2) After optimum polarization is obtained, turn off microwaves and 5 T magnet

(3) Use a 2nd magnet ($\sim$0.5 T) and very low temperatures to “freeze” the polarization (Frozen Spin Mode)

(4) Polarization will decay very slowly with a time constant of several days

(5) After polarization decays to about 50 % of its initial value, go back to step 1

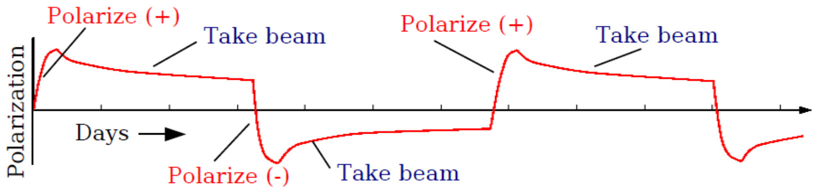

A Simple Way to Polarize

Brute Force Polarization

$$P_{\text{te}} = \tanh\left(\frac{\vec{\mu} \cdot \vec{B}}{kT}\right)$$

To get high polarization

maximize B

minimize T

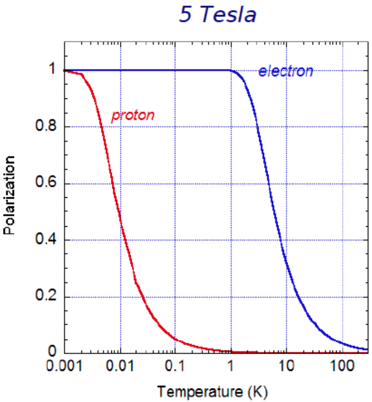

Disadvantages:

1. Requires very large magnet
2. Low temperatures require low luminosity
3. Polarization can take a very long time (protons slow, electrons fast)

A Better Way – Dynamic Nuclear Polarization

(1) Use brute force to polarize free electrons in the target material.

(2) Use microwaves to “transfer” this polarization to nuclei.

Mutual electron-nucleus spin flips re-arranges the nuclear Zeeman populations to favor one spin state over the other.

For best results:

DNP is performed at B/T conditions where electrons t_1 is short (ms) and nuclear t_1 is long (minutes):

$$\text{JLab: } B = 5\text{ T}, \quad T = 1\text{ K}$$

Materials for DNP Targets

Choice of material dictated by:

1. A maximum polarization
2. A resistance to ionization from radiation
3. A minimum number of polarizing nucleon

The holding magnet for FROST : 0.5 T

Compromise: Butanol (C_4H_9OH)

- Quality (dilution) factor:

  $f = \vec{N}/N_{\text{total}} = 10/74 \approx 0.13$

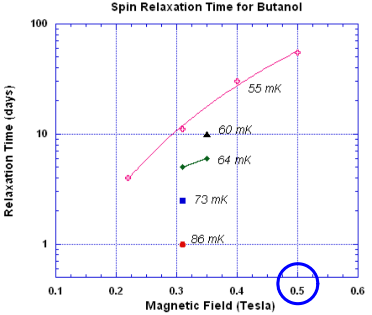

Ch. Bradtke, phD Thesis, Univ. Bonn, 1999

Refrigeration below 4.2 K - Evaporative Cooling

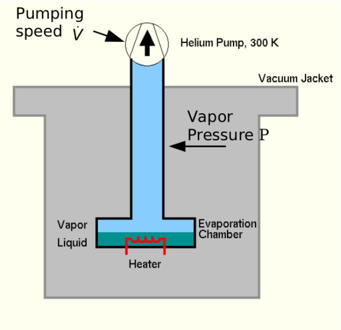

- In order to evaporate 1 mole of ^{4}He, the heater, L ($\sim$ 80 J/mol) must supply.
- In absence of a heater,
  - liquid will absorb heat from surroundings and liquid's temperature will drop
- Cooling power of a evaporation "fridge", $\dot{Q}$ is
  - $\dot{Q} = \dot{n}L = \dot{V}PL$

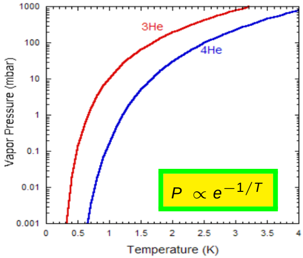

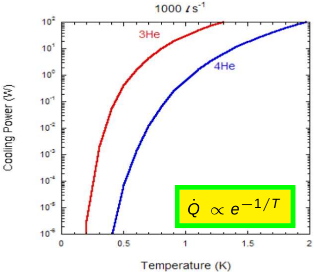

^{3}He/^{4}He Dilution Refrigeration

◇ Below 0.8 K, a ^{3}He/^{4}He mixture will reparate into two phases.

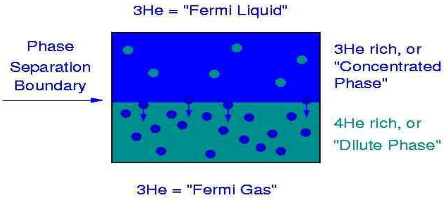

The specific heat of a ^{3}He atom

➜ C_c = 22 J/(mol·K)

➜ C_d = 106 J/(mol·K)

◇ The ^{3}He atoms move from the concentrated phase to the dilute phase with the heat energy exchange with the surroundings.

◇ Removing the ^{3}He from the dilute phase causes the ^{3}He atoms in the concentrated phase to

- absorb the heat from its surroundings
- dissolve into the dilute phase in order to re-establish a thermal equilibrium.

The ^{3}He/^{4}He Dilution Refrigerator for FROST

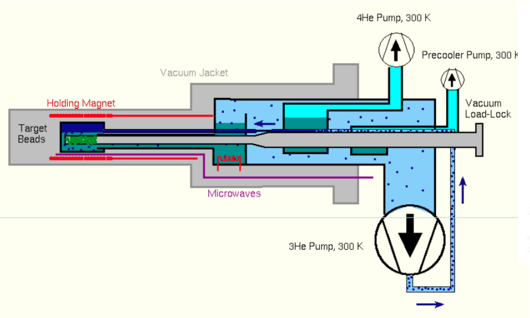

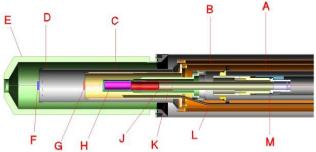

Figure 3.6: A cross section of the target area of FROST: *a)* primary heat exchanger; *b)* 1 K heat shield; *c)* holding coil; *d)* 20 K heat shield; *e)* outer vacuum can (Rohacell extension); *f)* polyethylene target; *g)* carbon target; *h)* butanol target; *j)* target insert; *k)* mixing chamber; *l)* microwave waveguide; *m)* kapton coldseal [10].

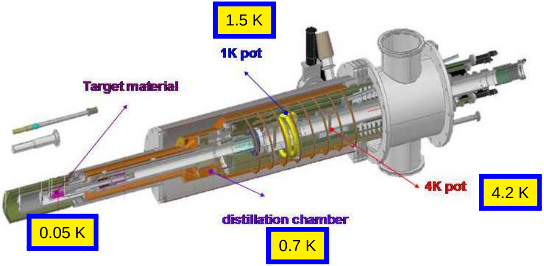

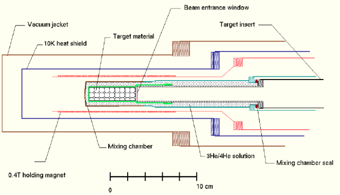

The Frozen-Spin Target - Summary of Results

	Expectation	Result
Base temperature:	50 mK	28 mK (w/o beam)
		30 mK (w/ beam)
Cooling Power:	10 μW (Frozen)	800 μW @ 50mK
	20 mW (Polarizing)	60mW @ 300 mK
Polarization:	80 %	+ 82 %
		- 85 %
1/e Relaxation Time:	500 hours	2700 hours (+ Pol.)
		1600 hours (-Pol.)

Lorentz Boost

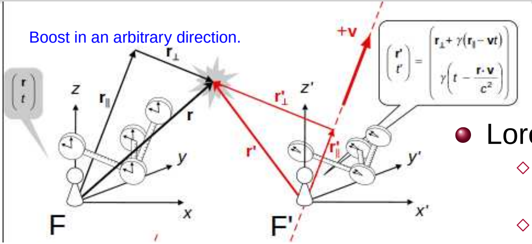

- Lorentz transformation
  - how measurements of space and time by two observers are related.
  - The Lorentz transformations are called "boosts" in the stated directions.

- The azimuthal angle, $\phi^*_{\pi^+}$ is calculated via two boosts.
  - The first boost along the beam line into the overall center-of-mass frame.
  - The second boost along the axis that is antiparallel to the recoiling proton.

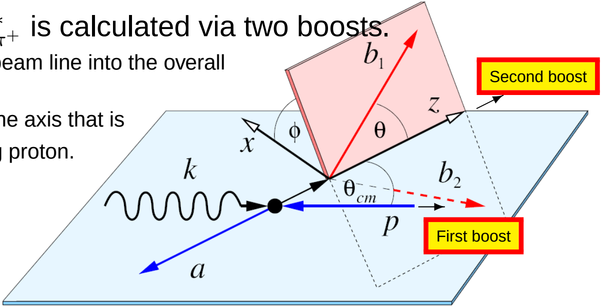

The voigt function

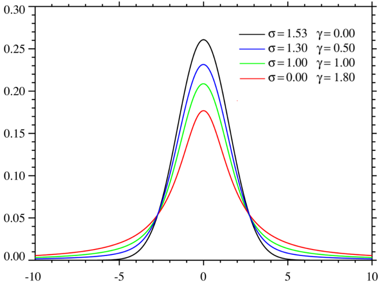

Voigt function

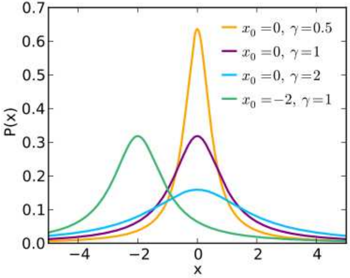

Breit Wigner function

- A voigt function, $V(x; \sigma, \gamma)$
  - A voigt function is a convolution of a Breit-Wigner function and a Gaussian function

$$V(x;\sigma,\gamma) = \int_{-\infty}^{\infty} G(x';\sigma) L(x-x';\gamma)\, dx'$$

  - $G(x;\ \sigma)$ is the centered Breit-Wigner function and $L(x;\ \gamma)$ is the centered Lorentzian functior

$$G(x;\sigma) \equiv \frac{e^{-x^2/(2\sigma^2)}}{\sigma\sqrt{2\pi}} \qquad L(x;\gamma) \equiv \frac{\gamma}{\pi(x^2+\gamma^2)}.$$

Hydrogen contamination of the carbon target (g9a)

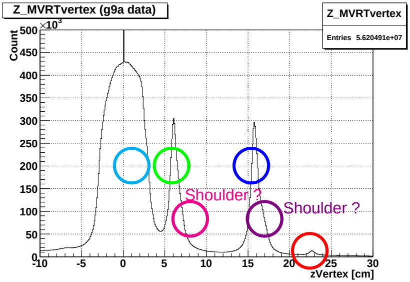

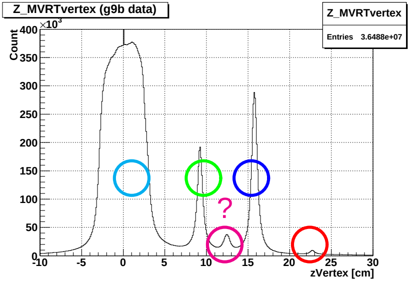

- The holding magnet for g9b is longer than for g9a

  so the carbon vertex for g9b is shifted into 3cm downstream

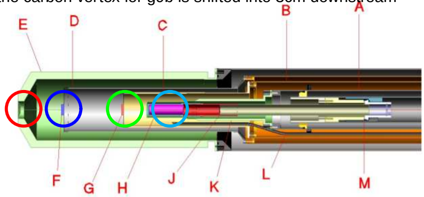

Figure 3.6: A cross section of the target area of FROST: *a)* primary heat exchanger; *b)* 1 K heat shield; *c)* holding coil; *d)* 20 K heat shield; *e)* outer vacuum can (Rohacell extension); *f)* polyethylene target; *g)* carbon target; *h)* butanol target; *j)* target insert; *k)* mixing chamber; *l)* microwave waveguide; *m)* kapton coldseal [10].

Hydrogen contamination of the carbon target (g9a)

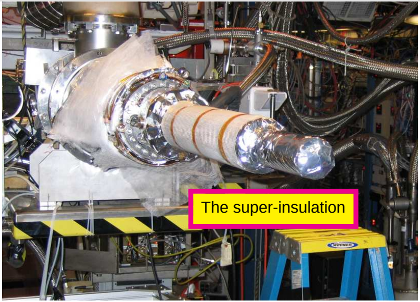

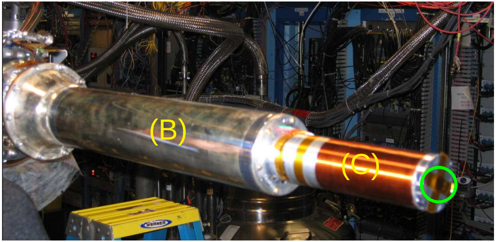

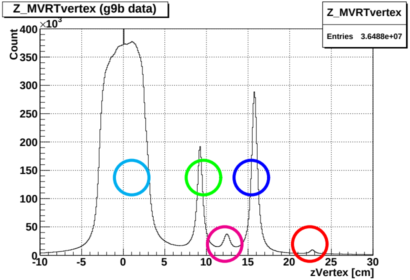

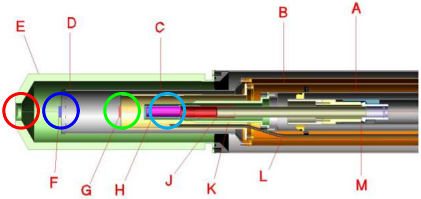

Figure 3.6: A cross section of the target area of FROST: *a)* primary heat exchanger; *b)* 1 K heat shield; *c)* holding coil; *d)* 20 K heat shield; *e)* outer vacuum can (Rohacell extension); *f)* polyethylene target; *g)* carbon target; *h)* butanol target; *j)* target insert; *k)* mixing chamber; *l)* microwave waveguide; *m)* kapton coldseal [10].

Hydrogen contamination of the carbon target (g9a)

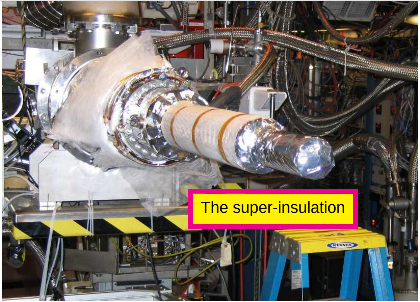

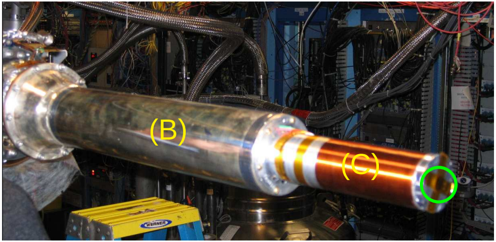

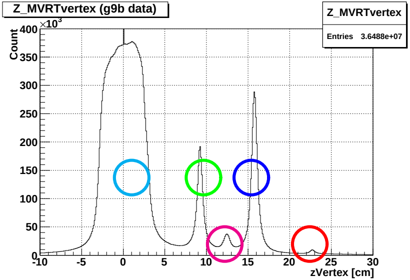

The conclusion :

- The shoulder near the carbon peak in g9a data and 12.5 cm peak in g9b are from super-insulation on the 1K heat shield
- The shoulder near the CH2 peak in g9a data is from super-insulation on the 20K heat shield
- The distance btw the carbon and super-insulation in g9a may be closer than in g9b
  - This make the carbon data contaminated by the hydrogen in g9a data

Proton and Pion Selection

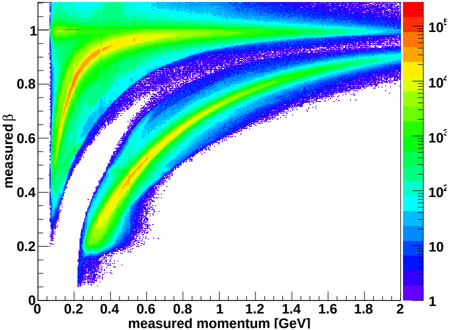

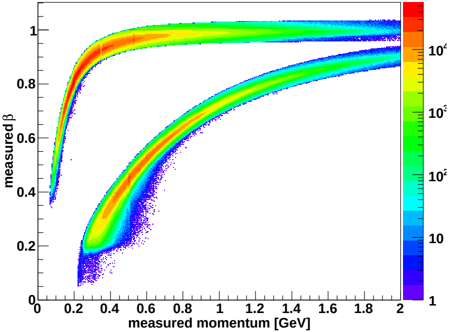

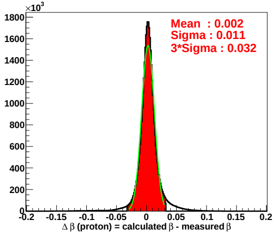

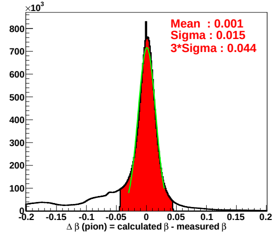

- proton selection
  : $|\,\Delta\beta\,| < 0.032$
- pion selection
  : $|\,\Delta\beta\,| < 0.044$

General method to get the phase space scale factor

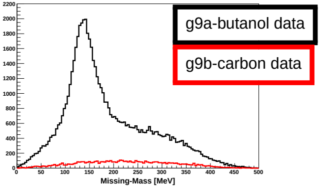

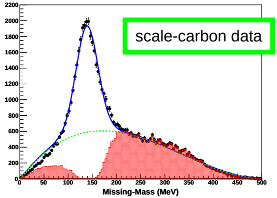

$$\text{scale factor} = \frac{\text{scale-carbon data}}{\text{g9b-carbon data}}$$

- The bound-nucleon events are isolated from the butanol data by a loose cut at

  $MM^2 < -0.2\,\text{GeV}^2$.

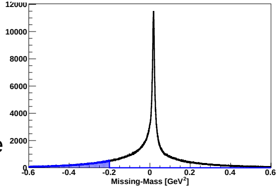

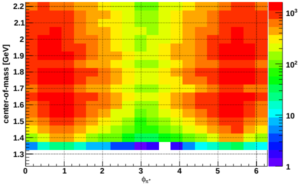

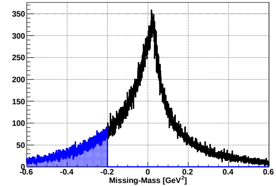

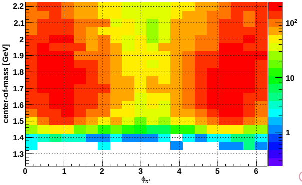

General method to get the scale factor

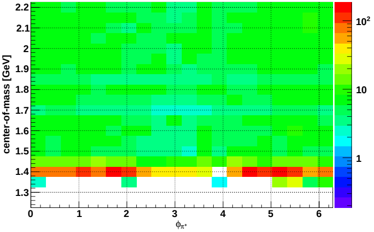

- The phase-space scale factor (W versus $\phi^*_{\pi^+}$)
- This scale factor is calculated by dividing two histograms. (Butanol/Carbon)

scale-carbon data

= scale factor X carbon data

free-proton data

= butanol data – scale-carbon data

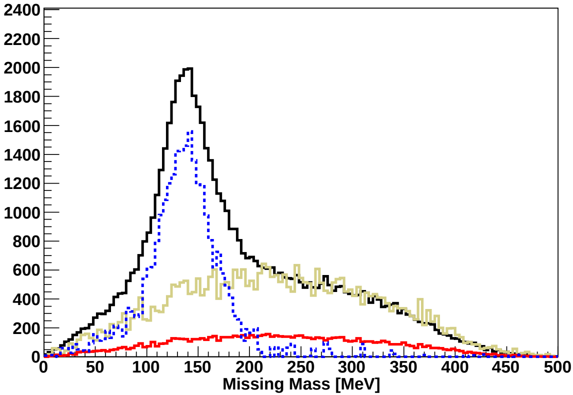

The internal conditions of the Q-factor method

◇ Optimizing the number of binning

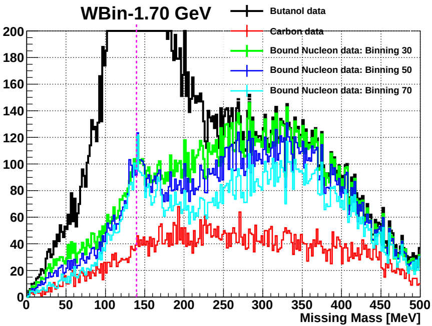

➜ the proper number of binning is 30.

◇ Optimizing the number of nearest events

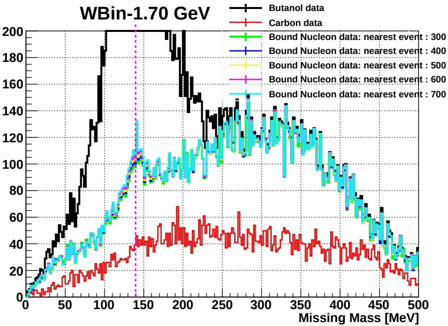

➜ the proper number of nearest events is 300.

Polarization observable $\mathbf{I}^{\odot}$

$$\mathbf{I}^{\odot}(\mathbf{W},\ \phi_{\pi^+}) = \frac{1}{\bar{\delta}_{\odot}(\mathbf{W})} \frac{\left\{ N(\rightarrow; \mathbf{W}, \phi_{\pi^+})_{beam} - N(\leftarrow; \mathbf{W}, \phi_{\pi^+})_{beam} \right\}}{\left\{ N(\rightarrow; \mathbf{W}, \phi_{\pi^+})_{beam} + N(\leftarrow; \mathbf{W}, \phi_{\pi^+})_{beam} \right\}}$$

- $\bar{\delta}_{\odot}(\mathbf{W})$: The average of the degree of the photon beam polarizations
- Λ_z : The degree of the target polarizations
- F : The photon flux (Normalization factor between periods)
- $\rightarrow$ ($\leftarrow$) : the direction of the beam polarization is parallel (anti-parallel) to the beam.
- $\Rightarrow$ ($\Leftarrow$) : the direction of the target polarization is parallel (anti-parallel) to the beam.
- Using the dataset with the unpolarized target and circularly-polarized beam

$$N(\rightarrow;\ \mathbf{W},\ \phi_{\pi^+})_{beam} = \frac{N(\rightarrow\Rightarrow; \mathbf{W}, \phi_{\pi^+})_{butanol}}{\Lambda_z(\Rightarrow)\cdot F(\Rightarrow)} + \frac{N(\rightarrow\Leftarrow; \mathbf{W}, \phi_{\pi^+})_{butanol}}{\Lambda_z(\Leftarrow)\cdot F(\Leftarrow)}$$

$$N(\leftarrow;\ \mathbf{W},\ \phi_{\pi^+})_{beam} = \frac{N(\leftarrow\Rightarrow; \mathbf{W}, \phi_{\pi^+})_{butanol}}{\Lambda_z(\Rightarrow)\cdot F(\Rightarrow)} + \frac{N(\leftarrow\Leftarrow; \mathbf{W}, \phi_{\pi^+})_{butanol}}{\Lambda_z(\Leftarrow)\cdot F(\Leftarrow)}$$

Missing mass distribution in several CL-cuts.

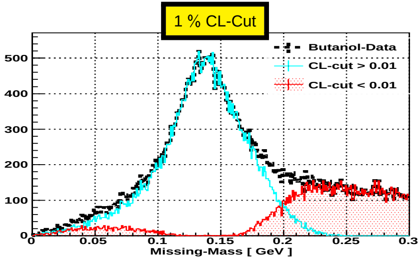

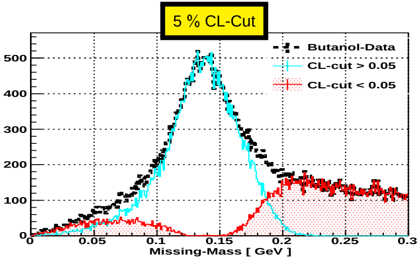

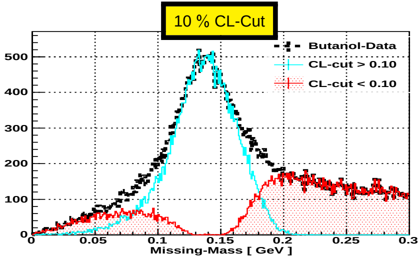

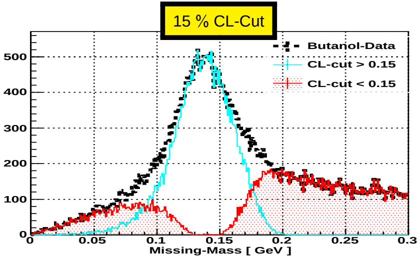

The background effect in Beam-Helicity Asymmetry $I^{\odot}$

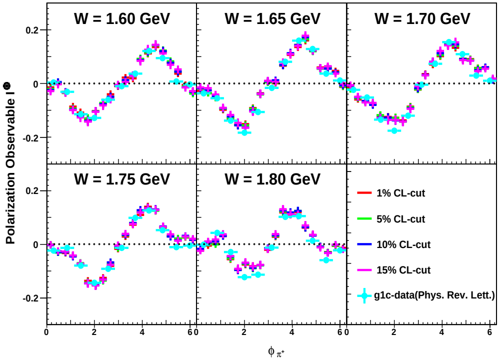

- The different CL-cuts have the different background effect. However, they have the similar values in the observable $I^{\odot}$.
- g9a dataset is not sensitive to distinguish between the beam asymmetry from free-proton, bound-nucleon and background data.